Figure 2:5 AGRG deployed a depth sounder on a canoe to survey the river bed elevations in the LaHave River upstream of Bridgewater.

Figure 2:6 River GPS and cross-section work upstream of Bridgewater.

Figure 2:7 River cross-section GPS survey upstream of Bridgewater on LaHave.

2.2. Lidar survey

The coastline of Lunenburg County was surveyed with lidar (Light Detection and Ranging) to produce a high-resolution Digital Elevation Model (DEM) in 2009 as part of the Atlantic Climate Adaptation Solutions (ACAS) project (Webster, McGuigan and MacDonald, 2012). In order to conduct a flood risk study for the Town of Bridgewater a lidar survey was conducted in May 11 and 12, 2012 by Leading Edge Geomatics (LEG) under contract to AGRG. In addition to the Town of Bridgewater, the Municipality of the District of Lunenburg and the NS Department of Transportation and Infrastructure Renewal also contributed to the purchase of the lidar which resulted in a survey area from New Germany to East LaHave where it overlaps the coastal lidar acquired in 2009 (Figure 2:8). The lidar was collected with a ground point spacing of ~ 1 m and covers the major floodplain of the LaHave River and the entire Town of Bridgewater. LEG performed their own internal quality assurance on the data by comparing 26 point locations obtained with survey grade GPS to the lidar and reported a vertical Root Mean Square Error of 5 cm and a 9 cm error at the 95% confidence interval. The lidar point data were classified as “ground” and “non-ground” by LEG and delivered to AGRG. Two surface models were constructed from these data; a Digital Surface Model which incorporates all the points and a bare-earth DEM which incorporates

only the classified ground points. The lidar vertical accuracy was independently validated by AGRG who also collected survey grade GPS measurements to test the accuracy of the lidar. GPS points were collected along the roadway for the length of the survey. The GPS points were compared with the lidar DEM and the difference in elevation was calculated. The mean difference between the DEM and GPS points was -0.05 m with a standard deviation of 0.06 m, which is consistent with the results of LEG. The lidar survey provides sufficient detail to model the floodplain but it does not penetrate the water surface, thus the fieldwork mentioned above was required in order to represent the river channel geometry.

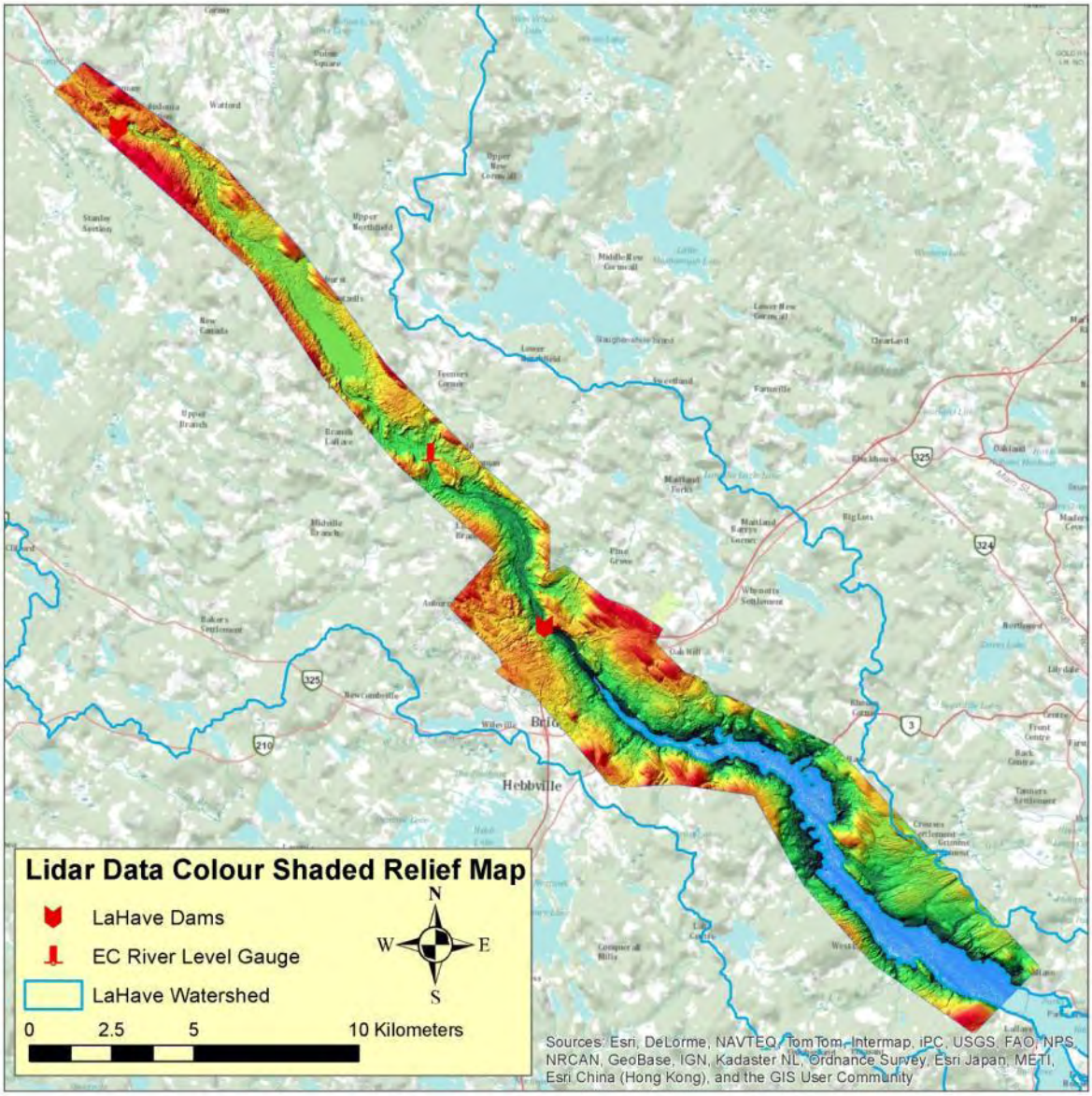

Figure 2:8 Extent of the lidar survey at 1 m resolution. Lidar survey conducted May 11 and 12, 2012.

2.3. Return Periods of Major Floods

2.3.1. Fluvial Flooding

The most common method to determine the return periods of extreme events, such as floods, is to use statistical methods to determine the probability of occurrence or return period of certain high water events. In this study we are examining the risk of flooding from two possible sources which can interact to compound the problem; river runoff from extreme precipitation or snow melt events, and storm

surges which elevate the tidal waters above usual levels. In order to calculate the risk of an extreme event occurring, a time series of events is used to examine how often such events have been used in the past. Webster, Mosher and Pearson (2008) used a Water Modeler software package to estimate the flood risk and probabilities of occurrence of storm surge high water events for Kingsburg. More recently Webster, McGuigan and MacDonald (2012) used a similar method to estimate the return periods for high water levels from the Halifax tide gauge and calculated the 100 year extreme water level under current conditions to be 2.2 m CGVD28. Hurricane Juan as measured at Halifax has a water level of 2.1 m which is very close to this 100 year return period level. The Halifax tide gauge is the nearest location of a long term record of sea-level for the study area and we have used the results from Webster, McGuigan and MacDonald (2012) to calculate return periods of storm surge high water events.

The time series of measured discharge of the LaHave River was used to determine the annual probability of extreme events and also the return period of certain high water events using a similar extreme value model approach as described above. The discharge record shows two extreme events, the major floods of 1956 and 2003. The time series record is examined to extract the annual maximum for each year (Figure 2:9).

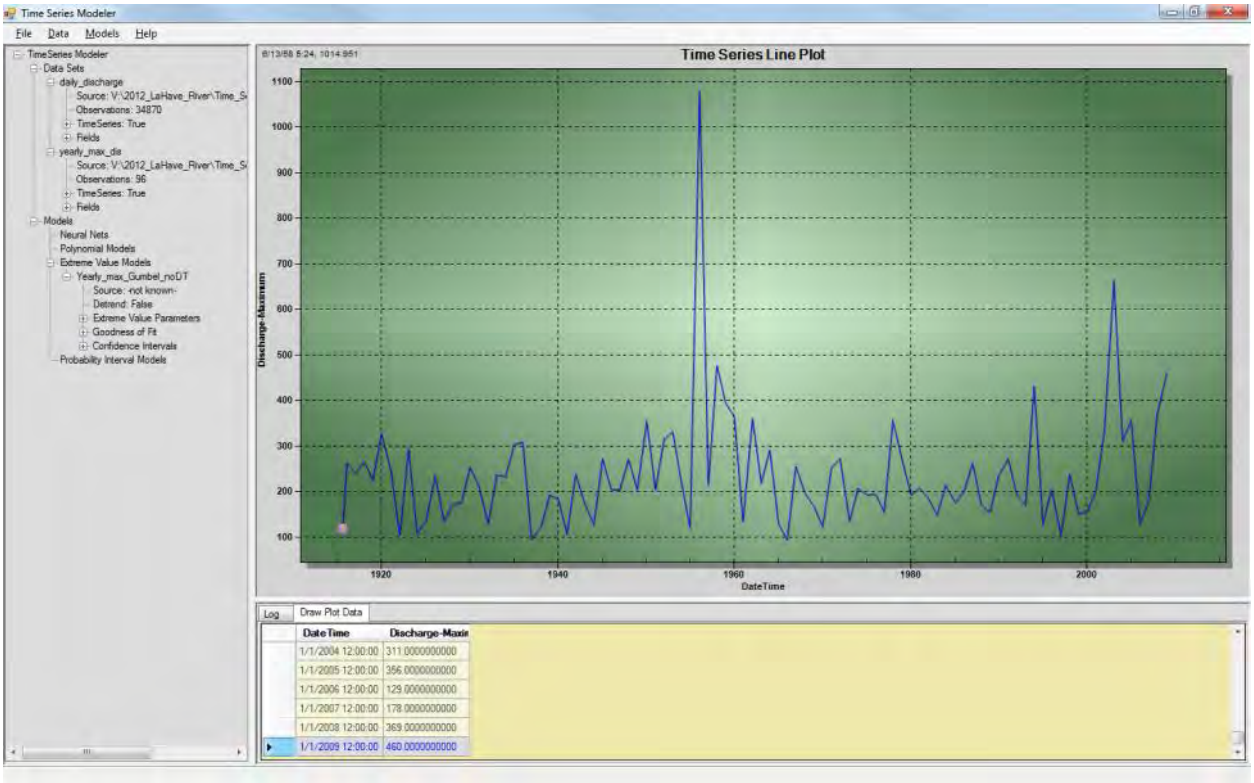

Figure 2:9 Time series of annual maximum discharge (m^3/sec) of the LaHave River from the Environment Canada gauge.

The annual maxima are then plotted and an extreme value model fitted to the distribution. Several models can be applied to the distribution (e.g. Logistic, LogNormal, Weibull, etc.); however the Gumbel Extreme Value Model (EVM) is one of the most commonly used. The empirical values, as measured by the Environment Canada gauge are plotted against the model values along with the model (line) and 95% confidence intervals (Figure 2:10). Statistics are reported in terms of the difference between the empirical and modeled values for the RMS error and correlation coefficient. We investigated the fit of several EVMs and selected the Gumbel distribution although it did not have the lowest RMS or correlation. Some models fit the overall distribution of events better but did not capture the extreme events, which is what we are most interested in. The Gumbel EVM line fell between the two most extreme flow events of 1956 and 2003 (red dots at the right of the graph, Figure 2:10) and best represented the extreme values.

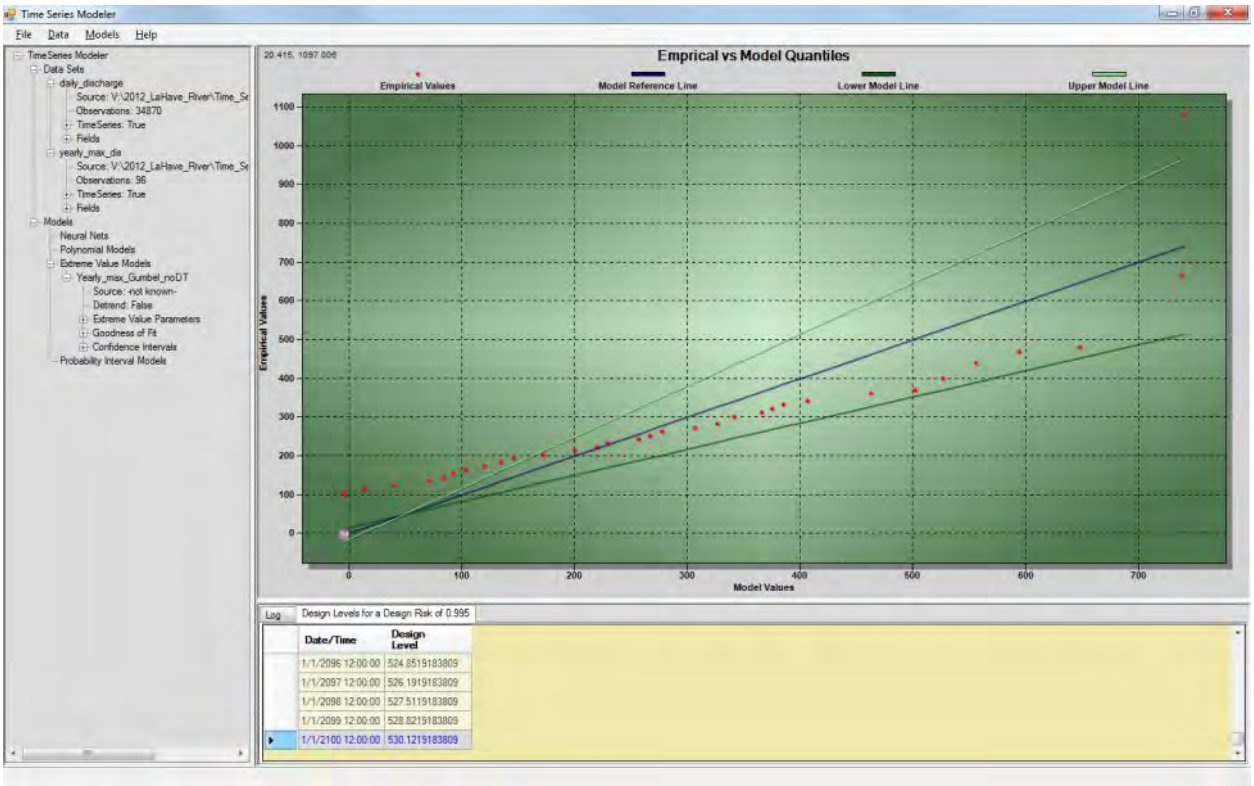

Figure 2:10 Plot of empirical (measured) and modeled extreme discharge events using a Gumbel extreme value model.

Once an EVM has been fitted to the data, the return period or annual probability of certain discharge volumes can be calculated or the discharge of the 50 and 100 year events be calculated. For example, the peak daily flow during the March 2003 flood on the LaHave River was 663 m^3/s and the discharge of the 1956 flood was 1080 m^3/s. We have used the discharge associated with the March 2003 event to

calculate the cumulative probability of the event reoccurring based on the EVM. The cumulative probability is also known as the design risk since risk must be considered when many structures are being designed. The X-axis represents the expected return period in years that such an event may occur and the Y-axis on the left side of the graph represents the probability of such an event occurring (0-1). The Y-axis on the right side of the graph represents the expected number of occurrences for a given return period or probability (Figure 2:11). The average return period for at least one occurrence of such an event, which for a Gumbel distribution is approximately 65%, is 53 years (demoted by the black vertical line Figure 2:11). The X-axis would have to be extended beyond 100 years to approach a probability near 1, currently the maximum probability approaches 0.85 which is equal to 1.9 expected occurrences of such an event within the next 100 years. Appendix 1 has a table which represents the graph in Figure 2:11 which has Date/Time, cumulative probability and the expected number of occurrences.

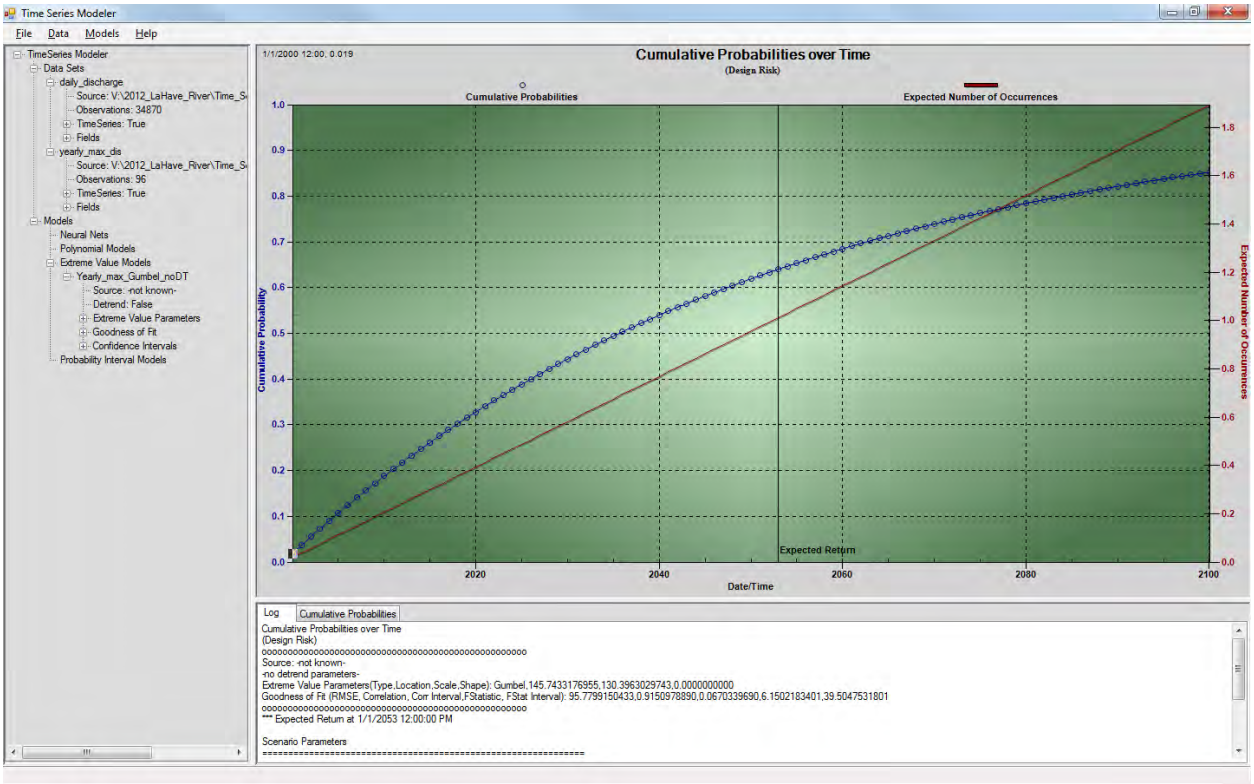

Figure 2:11 Design risk or cumulative probability of the March 2003 discharge event for the LaHave River. At least one event of this magnitude is expected to reoccur within the next 53 years. The X-axis is time from 2000 to 2100 representing 100 years. The Y-axis on the left side is probability and on the right side is expected number of occurrences.

The alternative approach to using the EVM to estimate risk is to set a fixed probability of occurrence and then calculate the discharge value for different return periods. This is the method used to estimate the

50 and 100 year return periods of extreme events. This approach is also known as the Design Level where structures must be designed to withstand a certain level (water level, weight etc.). If one chooses a probability of occurrence of 65% which equals at least one occurrence, then the design level can be calculated and the discharge for different return periods can be obtained (Figure 2:12). Thus for a 65% probability the 50 year discharge value (X-axis corresponding to 2050) is 652 m^3/s (Y-axis), whereas the 100 year return period corresponds to a 741 m^3/s discharge event. Appendix 2 has a table which represents the graph in Figure 2:11 which has the date/Time and Design level (discharge in this case).

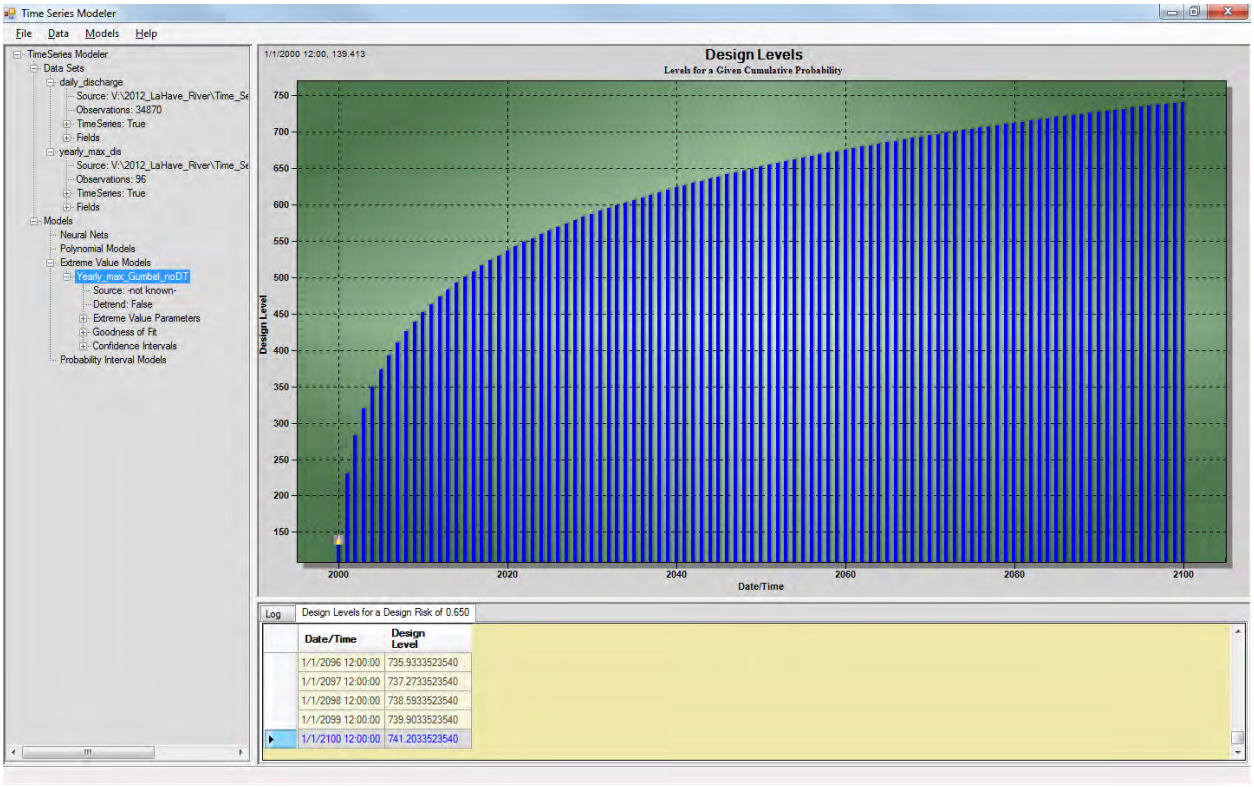

Figure 2:12 Design level for LaHave River discharge at a 65% probability. Return period on the X-Axis and design level (discharge m^3/sec) on Y-Axis.

Alternatively one can examine the design risk at a higher probability, such as 99.5% to determine how this will affect the design level for the 50 and 100 year return period as an example (Figure 2:13). With this higher probability the 50 year return event has a discharge of 441 m^3/sec and the 100 year event has a discharge of 530 m^3/sec. With the higher probability of occurrence the discharge is lower for a given return period.

It should be noted that when one states a return period of 100 years, it means that at least one or more occurrences are expected, depending on the probability used, within the next 100 years, not that it will

occur in 100 years or in the case of these graphs 2100. It should also be noted that extreme values are the toughest to model statistically since there are so few occurrences and thus these return periods and discharge levels should be used as a guideline and it should be understood there is a higher level of uncertainty when dealing with extreme event estimates. Table 2-1 summarizes the discharge event probability, return period in years and the associated discharge.

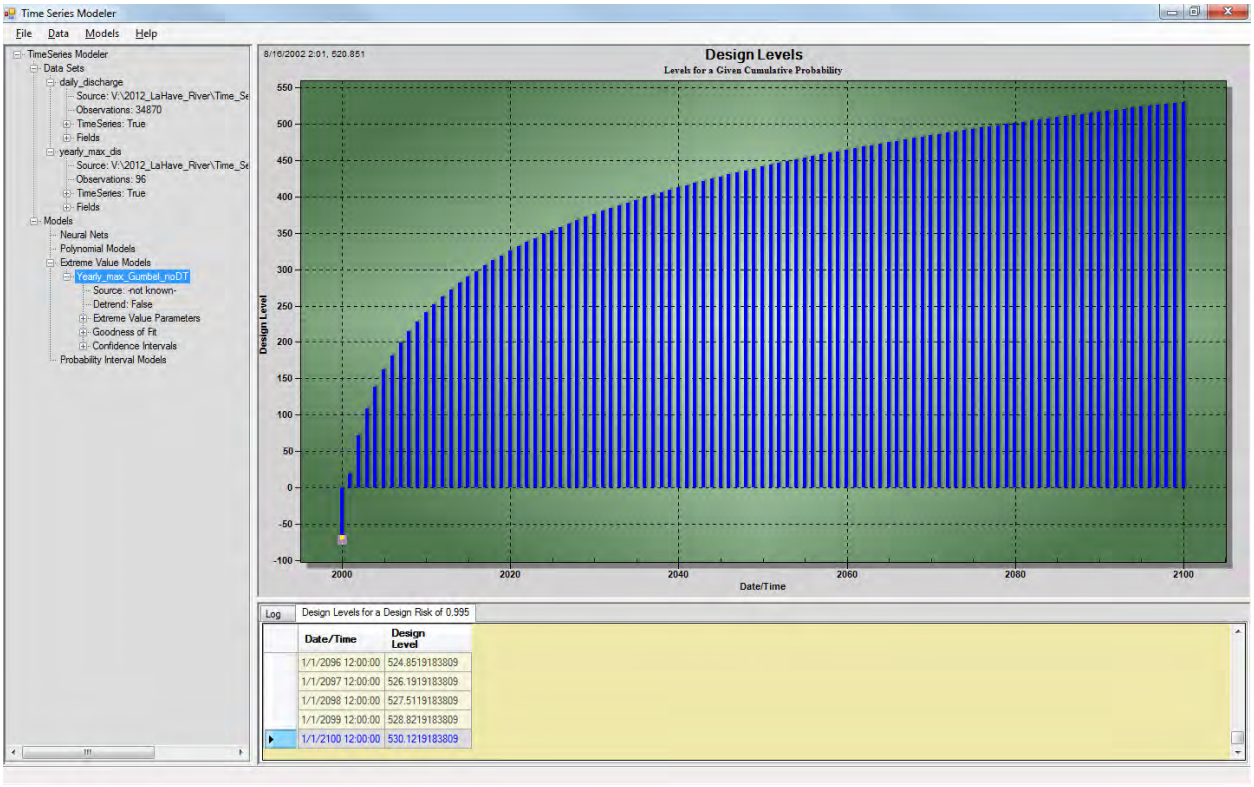

Figure 2:13 Design level for LaHave River discharge at a 99.5% probability. Return period on the X-Axis and design level (discharge m^3/sec) on Y-Axis.

Table 2-1 Return periods with 65% and 99.5% probability of the 50 and 100 year discharge events.

Event	Return Period in Years	Discharge (m^3/sec)
65% probability	50	652
65% probability	100	741
99.5 % probability	50	441
99.5 % probability	100	530

2.3.2. Storm Surge Flooding

In order to estimate the risk or probability of flooding related to high water events along the coast, we use a similar method as above to examine the Halifax tide gauge record. Note that the tide measurements have been left relative to chart datum (CD), which for Halifax is 0.8 m below CGVD28. Mean sea level has been rising in Halifax at a rate of 32 cm/century and the annual maximum water level has been increasing at a rate of 34 cm/century based on the best fit linear trend line of the tide gauge records (Figure 2:14). A Gumbel extreme value model was fitted to the distribution of the annual maximum water levels producing a correlation of 0.98 and a root mean square error (RMS) of 5 cm. The design level graph was calculated for a probability of occurrence of 95% to determine what water levels are expected over time (Figure 2:15). The design level graph provides answers to such questions as "What is the 100 year water level ?".

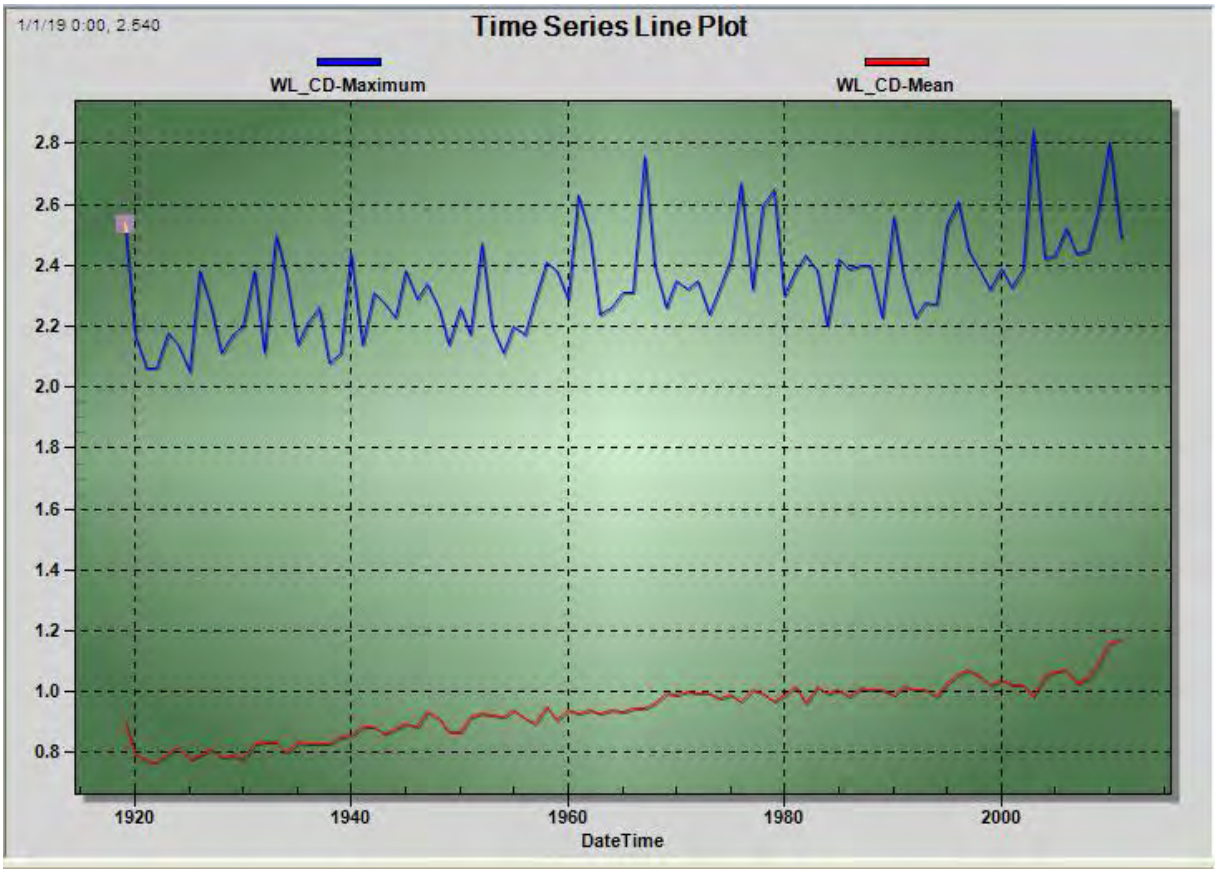

Figure 2:14 Halifax annual mean (red) and annual maximum (blue) water levels above chart datum for 1919 to 2010.

The one hundred year water level under current Relative Sea-Level (RSL - global sea-level rise and crustal subsidence) rise conditions is 3.03 m CD and increases to 3.32 m CD if RSL rises at a rate of 0.73 m/century (IPCC AR4) or further increases to 3.94 m CD if RSL rises at a rate of 1.46 m/century

(Rhamstorf) (Figure 2:15). The x-axis of Figure 2:15 represents return periods of water from 2010. The steep part of the curve, water levels as high as 2.4 m (CD) are expected to be seen within a return of 5 years (2015) regardless of the sea-level rise rate. The return period of water levels greater than 2.4 m (CD) are influenced by the sea-level rise rate. The expected water levels to be experienced over time at different RSL rates (current 32 cm/century, IPCC 73 cm/century and Rhamstorf 146 cm/century) for the Halifax extreme value Gumbel model are presented in Appendix 4.

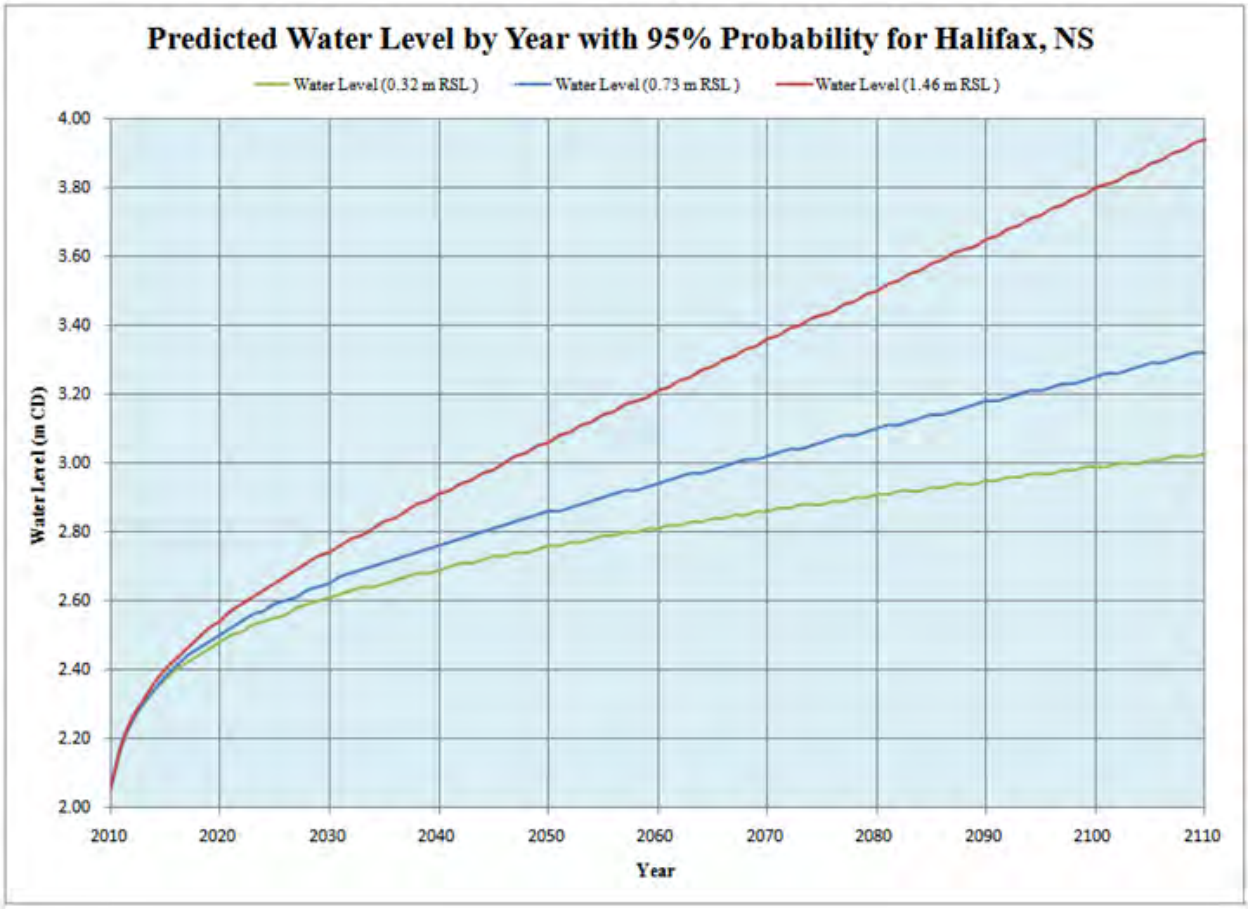

Figure 2:15 Design level graph for Halifax. Expected water levels to be reached over time with different rates of relative sea-level (RSL) rise (m/century), green – current rate 0.32, blue – 0.73 IPCC, red – 1.46 Rhamstorf.

The one hundred year return period water levels under different RSL conditions have been converted into the CGVD28 vertical datum for reference to the land DEM (note the water levels in figure 2.15 are referenced to CD). The 100 year flood level under current RSL conditions is 2.2 m, which is 10 cm below previous high water level maximum observed during Hurricane Juan in Halifax in Sept. of 2003 which had an associated storm surge of 1.63 m (Forbes et al. 2009). If RSL increases to a rate of 0.73 m/century, the 100 year water level increases to 2.5 m CGVD28 which further inundates areas. If RSL

increases to a rate of 1.46 m/century, the 100 year water level increases to 3.1 m CGVD28 which further inundates coastal areas.

2.4. Hydrologic Modeling

A high-resolution hydrodynamic model was developed using the DHI Mike21 software module to simulate tidal events. The bathymetry was represented by a grid which incorporated all of the depth sounding and coastline information (see Figure 2:4). The bathymetry grid and domain of the model extended from the mouth of the LaHave River to upstream of Bridgewater, the maximum extent of tidal influence. This two dimensional hydrodynamic model provided the linkage between ocean tidal predictions and inland tidal events by simulating water level variations and flows over modeled bathymetry in response to a forcing tidal boundary condition at the southern extent of the LaHave River. The boundary condition was developed using the ocean tidal predictions obtained from a global tidal model supplied by DHI which was used to predict ocean elevation along the Atlantic Coast. Once the bathymetry and boundary conditions were developed, a Mike21 hydrodynamic simulation (HD) was created and executed for calibration and validation purposes. Model results were extracted at the location of an AGRG tide gauge installed at Kraut Point. Comparisons were made between model predictions and gauge observations to establish proximal tide phase differences and elevation residuals caused by environmental factors.

A one-dimensional hydrodynamic model was developed using the DHI Mike11 for the LaHave River system from Bridgewater upstream to the Environment Canada water level gauge. In many studies of ungauged river systems, a watershed rainfall runoff model is developed to simulate the hydrological cycle within the area of study. This involves estimating parameters within the watershed that influence the amount of water that will infiltrate the ground versus runoff into the streams. In this study, however, since the LaHave River system has been gauged since 1915 and several major flooding events have been recorded, we have used the discharge record as a boundary condition for the Mike-11 river model. However, we did develop a watershed runoff model and calibrated it against the discharge as measured by Environment Canada. In order to have a sufficient time series of rainfall we used the Keji weather station record. However, for the final simulations we used the LaHave River discharge values to calculate the return periods of 50 and 100 year discharges under probabilities of 65% (at least one occurrence) and 99.5% probability as discussed in section 2.3.1. Once specific return period discharge values were calculated, hydrographs representing those discharge values were simulated and used as a boundary condition for the 1-D river runoff component of the model.

The Mike-11 and Mike-21 models were integrated and flood inundation maps were produced in Mike-Flood. In order to validate the results of the integrated model (Mike-11 and Mike-21) we compared our model results water levels with those measured at the Marine Terminal from the AGRG tide gauge. The tide gauge was located on the landward side of the wharf and we do not have accurate bathymetry representing this area as vessels were always tied up to the wharf during our bathymetric field surveys. In addition to the problem of a lack of bathymetric data, the channel between the wharf and land is relatively narrow and not well represented on our model grid, even at 3 m. As a result we extracted water levels from the model at a location close to the marine terminal in order to compare them to the observed water levels.

A nested grid approach was used allowing for concise transfer of mass and momentum across grid boundaries within the model domains, where the topography of the large area was represented by a 27 m grid which then was reduced by 1/3 to a 9 m grid around the Town of Bridgewater. This 9 m grid was further reduced by 1/3 to a 3 m grid to provide the most detail possible for generating the flood maps (Figure 2:16). As mentioned above, various boundary conditions were used including the river discharge and a tidal boundary (Figure 2:16).

The discharge measured at the Environment Canada gauge was supplemented with a proportion of additional discharge from two significant tributaries downstream of the gauge and prior to the town (Figure 2:16). A similar approach of scaling the discharge based on drainage area was used to determine the boundary condition for three streams within the town that are known to flood during heavy rainfall events. For the small streams within the town, only a Mike-11 model was used to generate flood extents based on cross-sections (Figure 2:16). In order to validate the flood extent maps for the streams within the town we simulated the May 22, 2005 flood event, using a proportion of the discharge observed in the LaHave River based on the drainage area of the streams. Since the hydrologic properties of the stream watershed are not necessarily the same as that of the LaHave River watershed, the discharge was amplified until the flood inundation matched the photographic evidence. A multiplication factor of three was eventually used so that the model results best matched the photo evidence. We used a combination of Google Street View and photographs supplied by the town showing areas of inundation (Figure 1:20 and Figure 1:21) to validate our model.

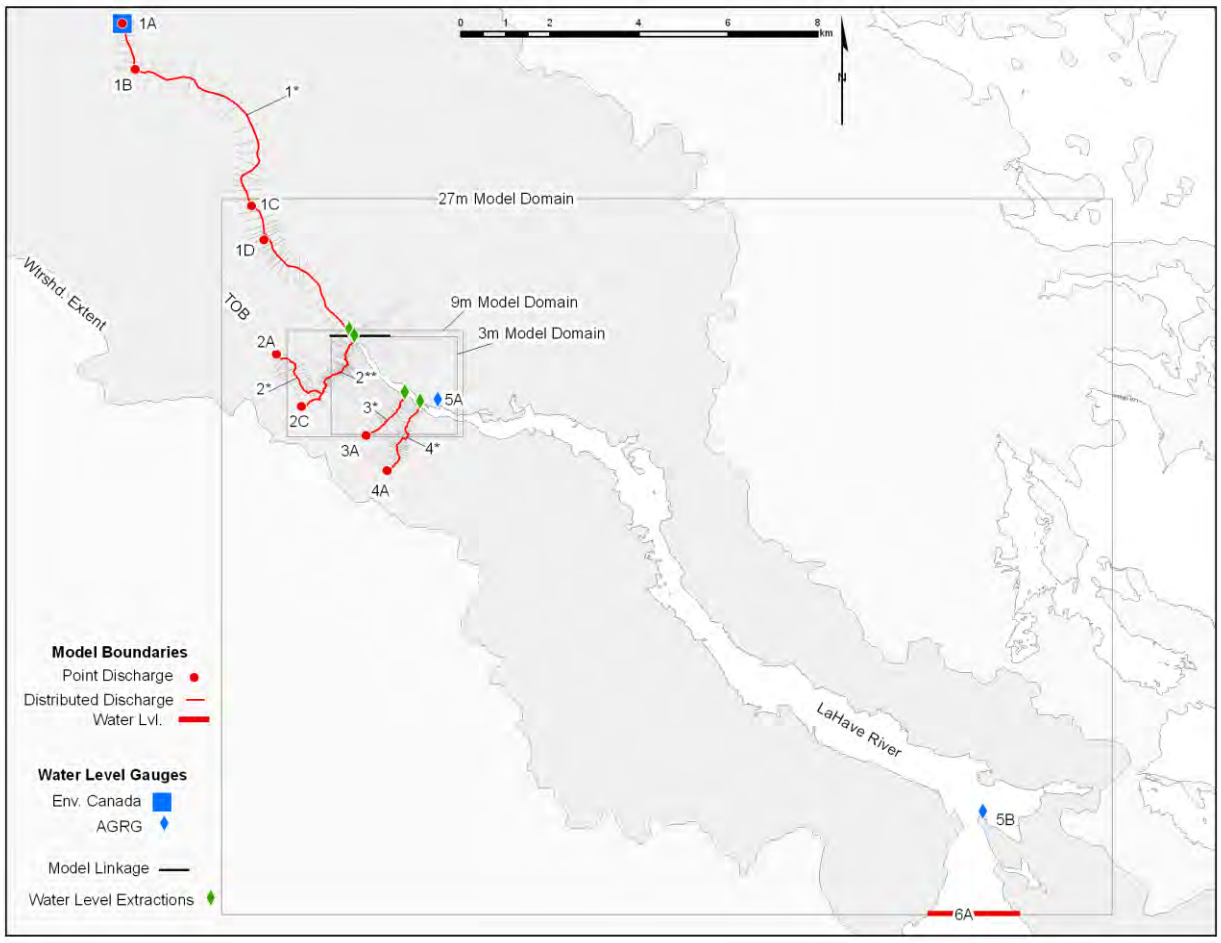

Figure 2:16 Map showing the nested grid model domain and location of boundaries, calibration and validation locations.

Three sets of model simulations were executed for the different return period discharges; one set based on variable discharge under normal conditions and two other sets based on variable discharge under different storm surge conditions (Table 2-2). Hydrodynamic simulations for the following conditions were generated:

Table 2-2 Model simulations. The * indicates a design risk scenario of 99.5% probability while ** corresponds to a design risk of 65% probability. Discharge values are applicable to the location of the Environment Canada LaHave River water level gauge.

LaHave River		**Tidal Condition**		
Scenario	Discharge (m^3/s)	Normal	Normal + 2.2 m	Normal + 3.5 m
50 year *	441	Simulation 50990	Simulation 50992	Simulation 50993
100 year *	530	Simulation 100990	Simulation 100992	Simulation 100993
50 year **	652	Simulation 50650	Simulation 50652	Simulation 50653
100 year **	741	Simulation 100650	Simulation 100652	Simulation 100653

The naming schemes of the simulations follows the format: the first 2-3 numbers indicates if it is a discharge return period of 50 or 100 years followed by the next 2 numbers which indicates the probability of occurrence being 65% or 99.5% followed by the last number which indicates the level of storm surge; 0 – normal high tide conditions, 2 for a 2.2 m surge on top of the predicted tide or 3 for a 3.5 m surge on top of the predicted tide. Initially we were going to model the March 31, 2003 event, however the recorded discharge of that specific event was 663 m^3/s which is very close to the 50 year return period at 65% percent probability (652 m^3/s).

To model a storm surge event in the order of 2.2 m, which is a major event in this region, the value of 2.2 m was added to the predicted tide level (Table 2-2). The selection of a 2.2 m storm surge was based partially on observations from the Halifax tide gauge where the storm surge for Hurricane Juan was measured at 1.63 m (it should be noted that this does not take into account waves). A larger value was selected in order to consider climate change and sea-level rise in the future. An additional set of simulations were executed with a 3.5 m storm surge at various river discharges (Table 2-2) in order to consider sea-level rise and the worst case scenario as outlined by Richards and Daigle (2012). The majority of the models were executed on the combined bathymetry and bare-earth lidar DEM. However, in order to evaluate the effect of buildings on the extent and movement of water we did construct one simulation using the building footprints and elevations imposed on the DEM. Flow velocities were affected, however the flood extents remained virtually the same, which for planning purposes was the focus of this study.

There were several boundary conditions used for the various simulations (Figure 2:17). We do not have an actual occurrence of peak discharge with peak storm surge; however this type of event is possible and thus was simulated for those models involving the storm surge components. The river discharge boundary condition was scaled proportionally to the drainage area for the LaHave River and for the streams and the storm surge was added to the predicted high tide (Figure 2:17).

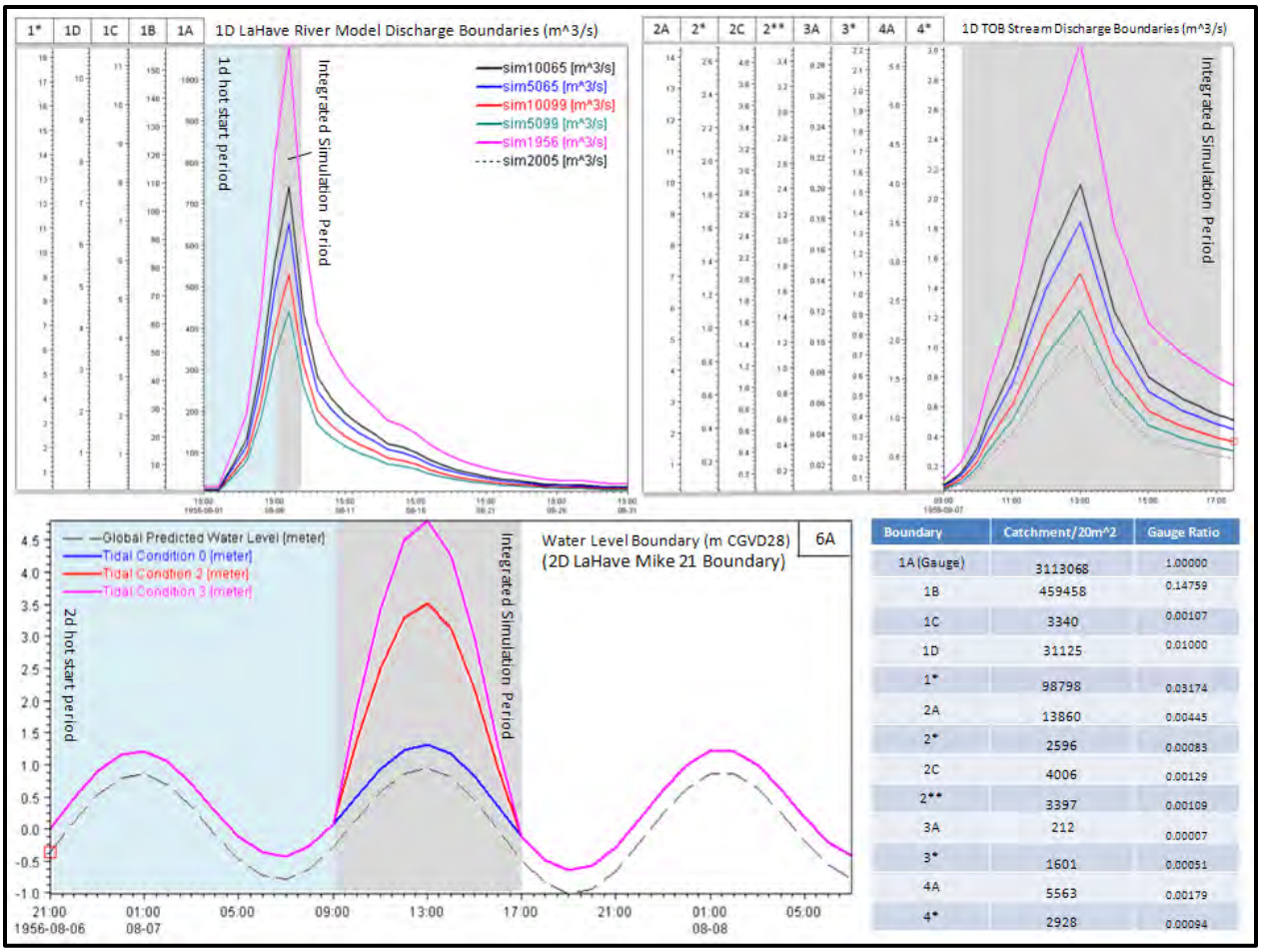

Boundary	Catchment/20m^2	Gauge Ratio
1A (Gauge)	3113068	1.00000
1B	459458	0.14759
1C	3340	0.00107
1D	31125	0.01000
1*	98798	0.03174
2A	13860	0.00445
2*	2596	0.00083
2C	4006	0.00129
2**	3397	0.00109
3A	212	0.00007
3*	1601	0.00051
4A	5563	0.00179
4*	2928	0.00094

Figure 2:17 Boundary conditions used for the various flood risk simulations. The number-letter reference for each panel and column refer to the location on the map in Figure 2.16. The blue shading in the graphs represents the start period and "warm up" of the model and the grey shading represents the time of the simulation and output. The blue shaded box denotes the stream river and stream boundary discharge values along with the ratio used (based on proportion of drainage area).

In many previous studies (Webster, McGuigan and MacDonald, 2012) of coastal flood risk mapping from storm surge events, a GIS based still-water approach was used. This involves raising the water level of the ocean as a horizontal plane interacting with the DEM. A further constraint was applied within the GIS environment to only flood low lying areas that are hydraulically connected with the ocean. The results of this method have been compared to actual flood extents and have shown good agreement (Webster et al., 2006). In this study we executed a still water model from 0-6 m in order to compare the extents derived from this simple GIS technique with those of the more sophisticated hydrodynamic modeling approach which accounts for river discharge and ocean circulation and surge.

2.5. Climate Change

Two factors have been considered when evaluating potential climate change and the effect on flood risk of the study area in the future. The first is with respect to how climate change is going to affect the drivers that influence watershed runoff events which include changes in precipitation and temperature. The second is with respect to sea-level rise as a result of the ocean warming and input of water from ice caps melting along with other sources. The sea-level rise component is further broken down into relative sea-level rise which is a combination of global sea-level rise and local crustal dynamics.

Climate model ensembles to produce averages of a variety of climate indices have been run to predict changes in the climate up to 2080 and reported by Richards and Daigle (2012) for communities in Nova Scotia and Prince Edward Island. They use 1980 as a base and make predictions for 2020, 2050 and 2080 of several climate variables including temperature, precipitation, water surplus and the intensity of short duration rainfall. The water surplus is defined as "The excess moisture remaining after the evaporation needs of the soil have been met (i.e. when actual evapotranspiration equals potential evapotranspiration) and soil storage has been returned to the water holding capacity level." These numbers are derived by using a water balance model. The surplus can be thought of as excess runoff. The deficit is water that could evaporate if it were available to do so. Water deficit is a drought indicator. The change in high intensity short duration periods rainfall is defined to be "Percentage change in the 20 year return value of the 24 hour precipitation currently used in building design." In general, climate models are considered accurate for predicting the mean changes of parameters but are less reliable for predicting extreme events such as the changes in short duration rainfall. Richards and Daigle (2012) state "Changes in intensity of extreme precipitation are difficult to predict. The consensus is that warmer climates are likely to experience an increase in precipitation intensity due to the relationship between saturated water vapour pressure and temperature. Global Climate Model simulations show that especially in areas where the mean precipitation is likely to increase, so is the probability of intense precipitation. Canada, and particularly eastern Canada, is in a zone of increasing annual precipitation." They also warn "It should be noted that estimation of changes to the frequency of extreme precipitation is a difficult and uncertain science at this point in time. These values are considered to be the best estimate from the published literature and may well be adjusted in the future as more information becomes available…. Information on the impact of climate change on short period rainfall rates is inconclusive at this point in time as there is no standard or accepted research methodology to determine how future sub-daily extreme rainfall could change in intensity and

frequency at point locations or over a small area in the future climate (Canadian Standards Association, 2010). Global and regional climate models operate at spatial and temporal scales which do not capture the small scale storms that are responsible for extreme short period rainfalls."

The annual changes in precipitation for the Bridgewater area have been extracted from Richards and Daigle (2012) in Table 2-3 along with the changes in a variety of other climate indices including water surplus and the intensity of short period rainfall (highlighted in yellow). Given the high degree of uncertainty in the parameters that will potentially affected flooding from runoff events, mainly the water surplus and the change in short duration precipitation events, we have decided not to generate a new set of model results for these predictions, but rather discuss the potential implications of return period of discharge events in the future in the discussion section of the report.

Table 2-3 Annual change in temperature and precipitation as well as other climate indices expected for 2020, 2050 and 2080, from Richards and Daigle (2012)

Parameter	1980s	2020s		2050s		2080s	
	Value	**Value**	**SD**	**Value**	**SD**	**Value**	**SD**
Temperature - Annual	6.8	8.0	0.4	9.2	0.6	10.5	1.0
Winter	-4.0	-2.7	0.6	-1.3	0.8	0.2	1.1
Spring	4.9	6.0	0.4	7.1	0.7	8.2	1.1
Summer	17.6	18.7	0.4	19.9	0.7	21.1	1.0
Autumn	8.7	9.9	0.4	11.0	0.6	12.3	0.9
Precipitation - Annual	1522.5	1564.2	37.4	1577.2	43.3	1624.0	56.6
Winter	436.2	457.5	17.3	468.4	22.3	493.9	28.6
Spring	392.4	405.4	16.5	411.2	22.3	427.3	29.3
Summer	294.4	299.3	17.4	298.4	23.2	298.8	38.3
Autumn	399.5	404.3	18.2	403.8	19.1	412.8	29.6
	1980s	**2020s**	**2050s**	**2080s**			
Heating Degree Days	4190.5	3847.0	3480.8	3127.0			
Cooling Degree Days	136.9	197.9	283.6	387.6			
Hot Days (Tmax > 30)	5.8	12.6	21.6	31.4			
Very Hot Days (Tmax > 35)	0.0	0.5	1.2	2.6			
Cold Days (Tmax < -10)	3.1	2.3	1.0	0.5			
Very Cold Days (Tmax < -20)	0.0	0.0	0.0	0.0			
Growing Degree Days > 5	1828.8	2055.8	2327.1	2628.8			
Growing Degree Days > 10	940.7	1102.9	1299.5	1515.9			
Growing Season Length (days)	160.3	174.5	191.9	213.5			
Corn Heat Units (CHU)	2518.5	2809.7	3144.2	3495.3			
Corn Season Length (days)	133.8	142.5	153.4	164.9			
Freeze Free Season (days)	195.6	222.5	243.8	263.1			
Days With Rain	138.1	147.1	150.9	154.0			
Days With Snow	36.1	51.7	43.9	37.1			
Freeze-Thaw Cycles - Annual	117.6	108.7	95.6	82.7			
Winter	45.5	45.9	46.2	44.9			
Spring	42.2	37.8	30.6	24.3			
Summer	0.6	0.4	0.0	0.0			
Autumn	29.3	24.6	18.8	13.7			
Water Surplus (mm)	1157.1	1004.5	978.1	982.7			
Water Deficit (mm)	31.5	35.8	44.0	53.1			
Δ Intensity Short Period Rainfall (%)	0	5	9	16			

Richards and Daigle (2012) also predict total sea-level rise for the 10, 25, 50 and 100 year return periods for the years 2000, 2025, 2055, 2085 and 2100 (Table 1-1). They make use of a storm surge model driven by historic winds and pressure fields every 6 hours and compare the water levels to predicted tide to calculate residuals (differences between predicted water level and that from the storm surge model)

(Table 1-1). This provides them with the residual water level for the 10, 25, 50 and 100 year return periods which they add to the predicted Higher High Water Large Tide (HHWLT) for Lunenburg to estimate a total water level. It should be noted that the water levels they report are referenced to chart datum and not the land datum used in the flood modelling CGVD28. They use a global sea-level prediction from Rhamstorf (2007) where they fit four median sea-level points for 1990, 2050, 2075 and 2100 with a second order non-linear polynomial. They then extracted the global sea-level for 2025, 2055, 2085 and 2100 from this curve. They use a crustal subsidence estimate of 15 cm by 2100 to calculate total sea-level rise predictions. However, because of the storm surge model output they are using they state "The estimated extreme total sea levels were calculated as the sum of the 10-, 25-, 50- and 100-Year return period residuals (from the Bernier method) and the HHWLT values for the future time frames of 2025, 2055, 2085 and 2100. These estimates do not include the impact of an extreme historical event such as the Saxby Gale (1869), the Groundhog Day Storm (1976), a direct-hit by a hurricane (i.e. Hurricane Juan 2003) or similar extreme past or future meteorological events. From a precautionary principle approach to risk management it is advisable to consider the impacts of a plausible upper bound water level that would combine the upper limits of global sea-level rise, local crustal subsidence and the highest storm surge factor previously recorded by a tide gauge, or where available, some high precision measurements of identified high water marks."

Thus in addition to their projected total sea-levels which may not reflect events such as hurricanes, they also produced a set of water levels that represent a plausible upper limit which combined the highest predicted tide (HHWLT), total sea-level rise including the upper error bar estimate, with the maximum storm surge recorded by the nearest tide gauge. In the case of Lunenburg, the largest storm surge was 1.63 m recorded during Hurricane Juan in 2003 (Table 2-4).

Table 2-4 Plausible upper bound water level for year 2100 calculated as the sum of: current HHWLT, predicted sea-level rise plus error bar, and the maximum storm surge recorded to date.

CHS Representative site	HHWLT m (CD)	Sea-Level Rise (2100) + Error Bar (m)	Maximum Storm Surge to Date (m) (See Note 1)	Plausible Upper Bound Water Level (m) (CD) by Year 2100 (see Note 2)
Lunenburg	2.43	1.54	1.63	5.60

As described earlier in this section Webster, McGuigan and MacDonald (2012) analyzed the Halifax hourly tide gauge record from 1919 to 2010 to calculate return period water levels. This method does

capture short term event water levels such as those from hurricanes, including Juan. They have then produced return periods and water level scenarios under three relative sea-level rise possibilities (current situation, IPCC estimate and a Rhamstorf et al. estimate) assuming a linear increase in sea-level to 2100.

The difference in these approaches produces slightly different water levels. We have decided to model the risk of flooding using variable discharge rates under a normal tide conditions (maximum high tide in a year) and with a 2.2 m and a 3.5 m storm surge. The results of these simulations allow us to extract various water levels that have been predicted using these methods and will be discussed later in the discussions section of the report.

2.6. River Bank Erosion Assessment

In order to assess the degree of erosion of the river bank adjacent to the Town of Bridgewater, a series of historical aerial photographs were scanned, orthorectified and the coastline interpreted. AGRG subcontracted this work to GeoNet technologies who delivered the orthophotos, coastlines and rate of change coastlines between 2009 and the previous dates of imagery. The historical aerial photos could be a valuable addition to the town's GIS layers. In addition, the photos provided a means for delineation of the riverbank edge, and the ability to measure change over the years from the different photos.

The orthorectified images will also be valuable in identifying infrastructure and other assets that existed along the riverbank throughout the years. This could be valuable from a historical and heritage perspective, as veteran residents would be able to identify changes and recall the reasons – flood, fire, replacement, etc. GeoNet initially received numerous photographs from the Town of Bridgewater, for the years 1948, 1965, 1967, 1992, 2001, and 2009. The photographs received for 2009 were already rectified and were not involved in the orthorectification process directly. After a review of the earlier years of photography, 46 photographs of varying years were selected and scanned at 600 dpi. Upon receiving the project boundary (town boundary) after the scanning, it was determined that 30 photographs would be sufficient to cover the study area and used in the orthorectification process. Since no camera calibration reports were provided and in some cases fiducial marks on the photographs were missing or degraded, manual measurements were taken or approximated and fed into the orthophoto production software. Available topographic data (masspoints, roads) were used to create the DEM necessary for the orthorectification process.

The existing 2009 orthophotos and existing vector data were used for selecting photo control. When possible, road intersection, building corners and other common features were used to pick ground control points for the various years. At this stage, residual values calculated by the software were monitored to ensure the best control was picked. However, in some cases, especially in the earlier years, finding good control was difficult. Reviewing the residual error values, overlaying the existing vector data and comparing the fit between adjacent images of the same and varying years made up the quality control process.

The traditional Geomatics definition of the shoreline is defined as the mean high water line. This is often very difficult to determine and is often demarcated by the wrack line observed on aerial photographs representing sea-weed and other debris deposited along the shoreline. In terms of shoreline change detection (erosion or accretion) this definition is not appropriate as consistency between temporal aerial photos is challenging. Instead, the term coastline is often used to mean the higher high water extent or from a geomorphological perspective, the most land-ward influence of the ocean. It is in this context that "coastline" was used to map the change over time of these features. Change along the coastline is defined as the difference in lateral position of the coastline between two dates in time in a direction perpendicular to the coastline. The rate of change along the coastline is defined by the quotient of the latter change in meters of the coastline position divided by the time difference of the orthophotos of which the coastlines were derived. The rate of change in this project was expressed in both metres/year and feet/year along the coastline. Where possible the following guidelines for coastline position were adhered to for the delineation exercise:

1. At the top of steep embankments

2. The beginning of terrestrial vegetation.

3. In low-lying marshy areas where coastline definition isn't so clear, tonal differences in the imagery were used as a guide for plotting the coastline.

An example of the historical orthophotos and interpreted coastlines in shown in Figure 2:18.

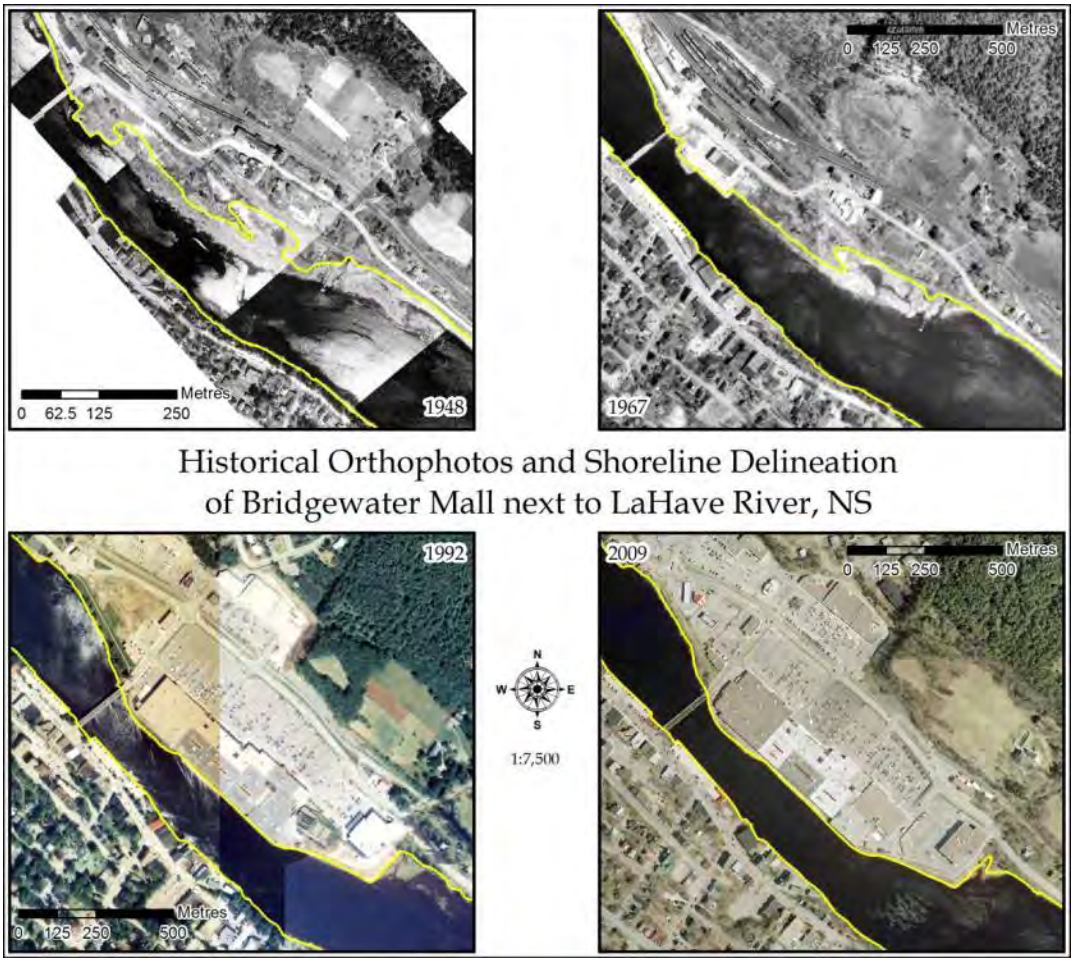

Figure 2:18 Historical orthophotos and shoreline delineation (in yellow) from 1948, 1967, 1992, and 2009 of the mall and the LaHave River in Bridgewater, NS.

The dates of the photographs were problematic to determine and are shown in Table 2-5. The photos taken in 2009 to which each other dataset was compared show leaf-off conditions, whereas there are leaf-on conditions in the rest of the aerial photos (Figure 2:19). This indicated the photos were taken in early spring or late fall, though there are no signs of snow, however the water levels are traditionally high at both these times of year.

Table 2-5 Dates of the aerial photographs used in the coastline change study.

Bridgewater Riverbank Study - Photograph Dates

YEAR	Photographs	Date (as printed)	Notes
1948	All	No date on scanned image.	Date may be on backside of print. Sent back to client.
1965	All	6-7-65	
1967	All	No date on scanned image.	
1992	92335-160	92-07-16	

"	92335-161	92-07-16	
"	92338-015	92-07-16	
"	92339-048	92-07-17	
2001	All	01-08-26	
2009	All	No date on scanned image.	Rectified images supplied by client. Date should be on print.

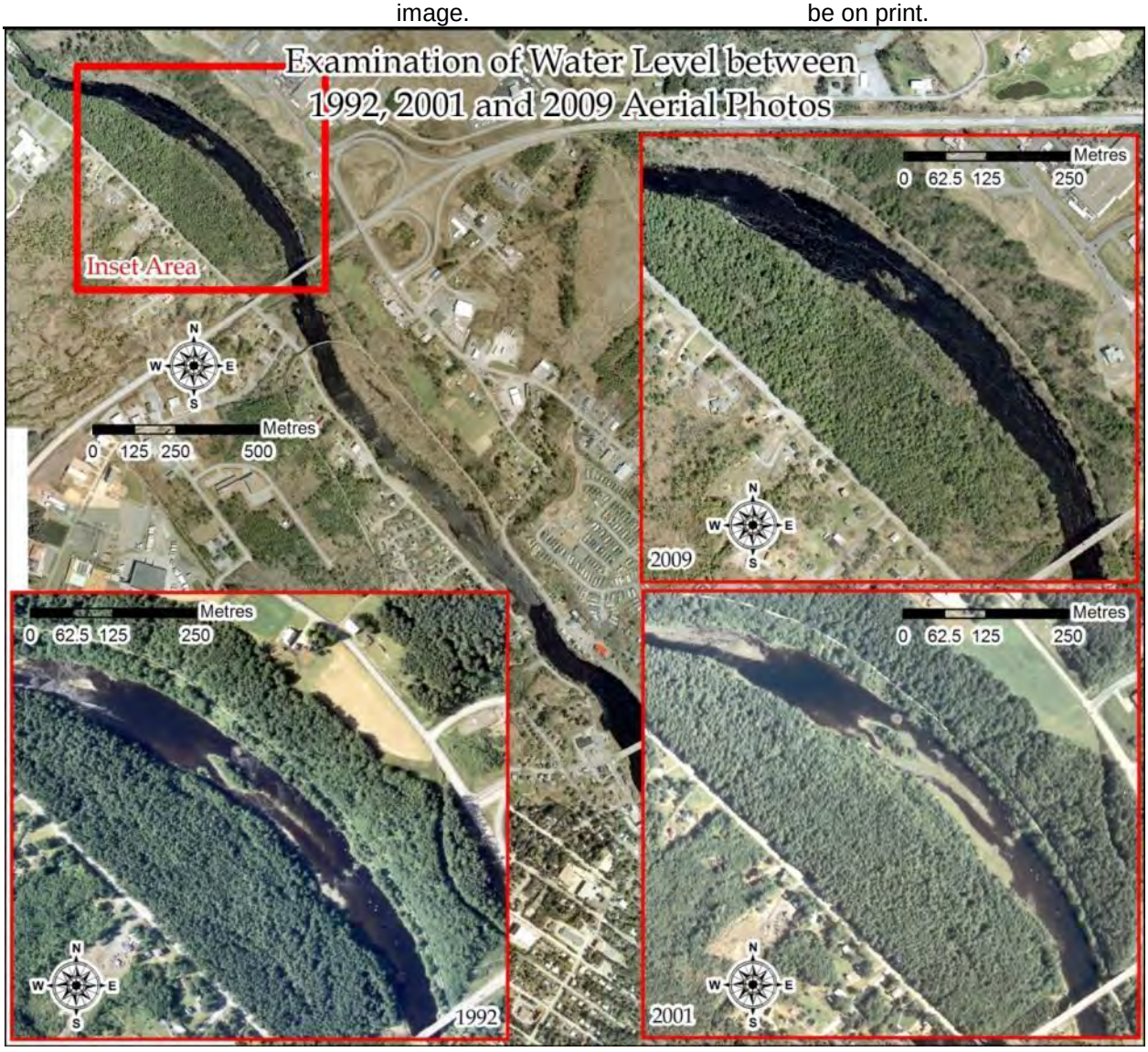

Figure 2:19 Photos taken at different times of the year may have variable water levels in the river, adding complications to the river bank interpretation.

The vector coastlines were interpreted from each photograph and then spatial analysis was performed to calculate the shortest distance between the lines. The 2009 coastline was then segmented every 1 m and the distance value assigned as an attribute. The rate of change was then calculated as an additional attribute by dividing the distance of change by the time span in years between the photos. Thus, a

yearly rate of change coastline vector was calculated for each time period and the reference 2009 coastline.

3. Results

3.1. Field Instrumentation

The data were downloaded from the various instruments deployed by AGRG in September and in mid-December, 2012. The weather station data was used to supplement the calibration of our rainfall runoff model which was initially based on the rainfall and temperature obtained from the Keji weather station. The engineering department for the Town of Bridgewater also supplied us with weather station data which was compared to the AGRG weather station deployed at Hirtles Beach (Figure 3:1).

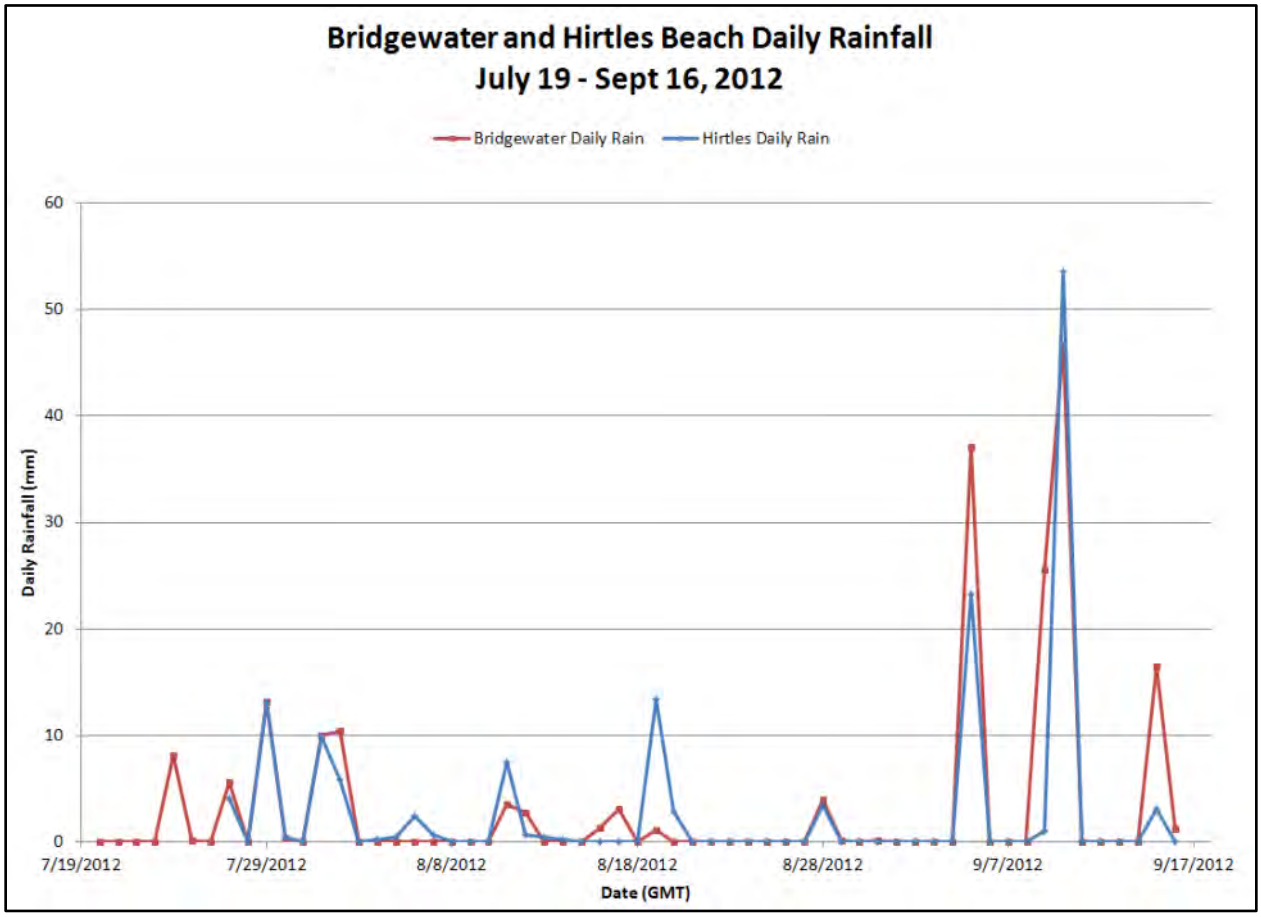

Figure 3:1 Comparison of daily rainfall measured at Bridgewater station versus Hirtles Beach.

Since the LaHave watershed is so large and there is a significant catchment area upstream of Bridgewater we also deployed a weather station at Cherryfield near Springfield. Unfortunately the station was vandalized and we did not get a complete record. However we did get the station operating again in November and have compared the rainfall events at Hirtles and Cherryfield (Figure 3:2).

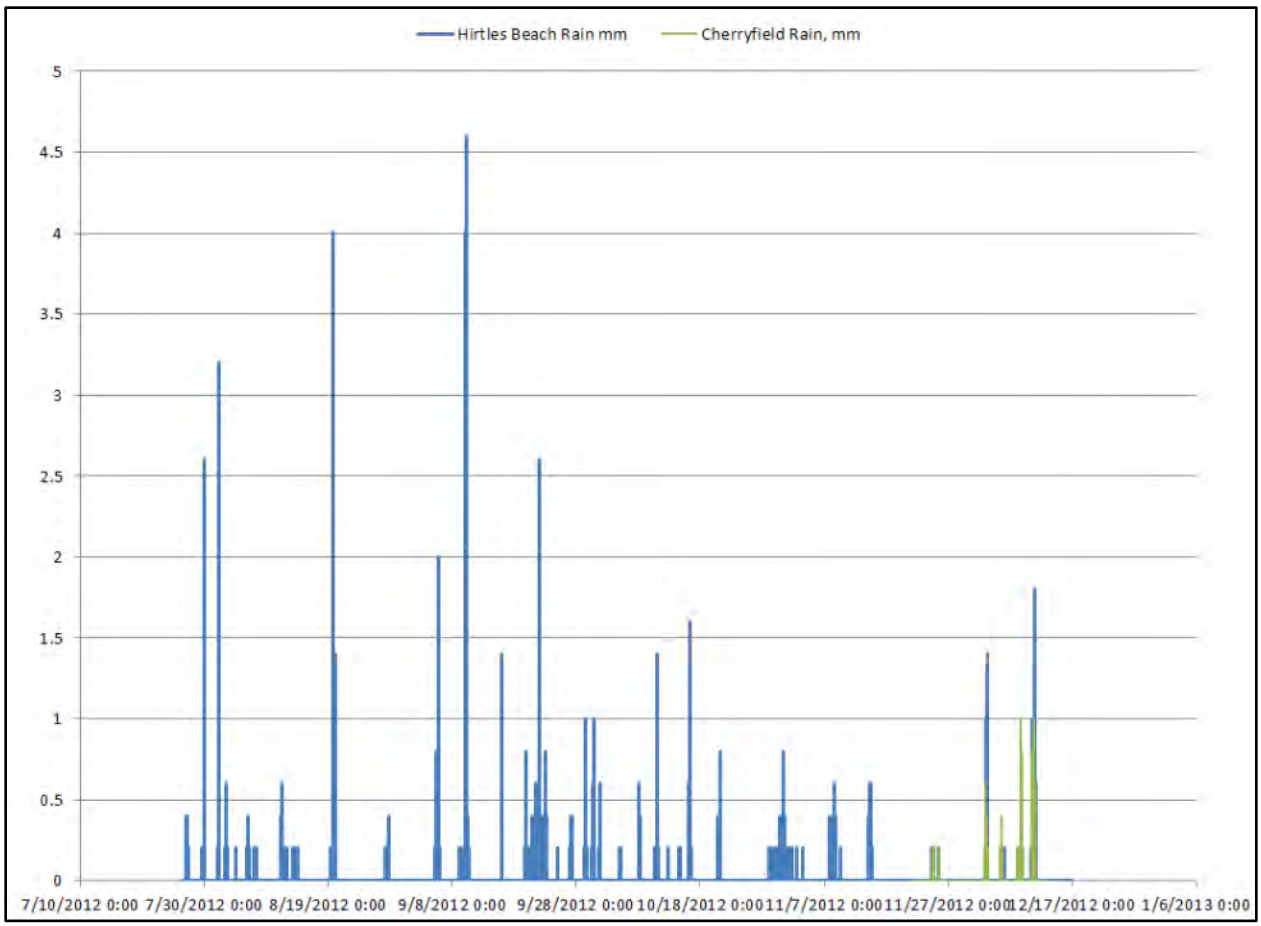

Figure 3:2 Comparison of hourly rainfall measured at Hirtles beach versus Cherryfield.

These various weather station records have been used to refine the initial parameters of the watershed rainfall runoff model. Our longest record is from the Hirtles Beach weather station that will be deployed there on a semi-permanent basis to observe coastal conditions (Figure 3:3).

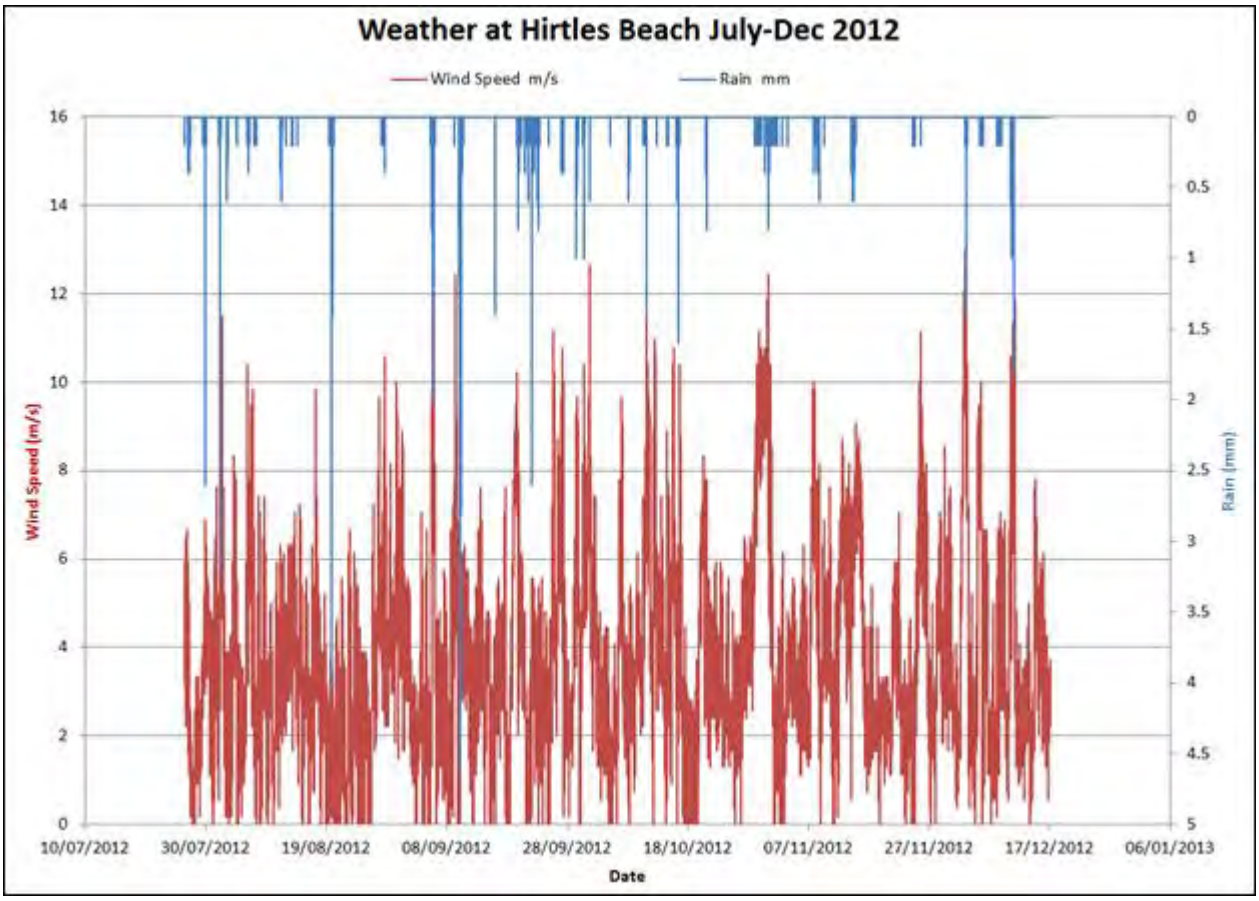

Figure 3:3 Hirtles beach weather station example plot of wind speed and hourly rainfall, July-Dec. 2012.

The tide gauges deployed at Kraut Point and at the Marine Terminal in Bridgewater were used for two purposes. One was to ensure that our tidal boundary condition, which is based on the predicted tide, was accurate and the other was to observe the water level and record any storm surge events. The Kraut Point tide gauge will remain deployed for the winter of 2012-2013. In both cases the pressure sensors were not deployed low enough to capture the lowest tide and the readings "bottom out", however it is the high water events that concern us and these were captured. The predicted tide was obtained from (http://tbone.biol.sc.edu/tide/) for Bridgewater and Riverport which is very close to Kraut Point (Figure 3:4). It was observed that the tide is predicted to be higher in Bridgewater than at Riverport.

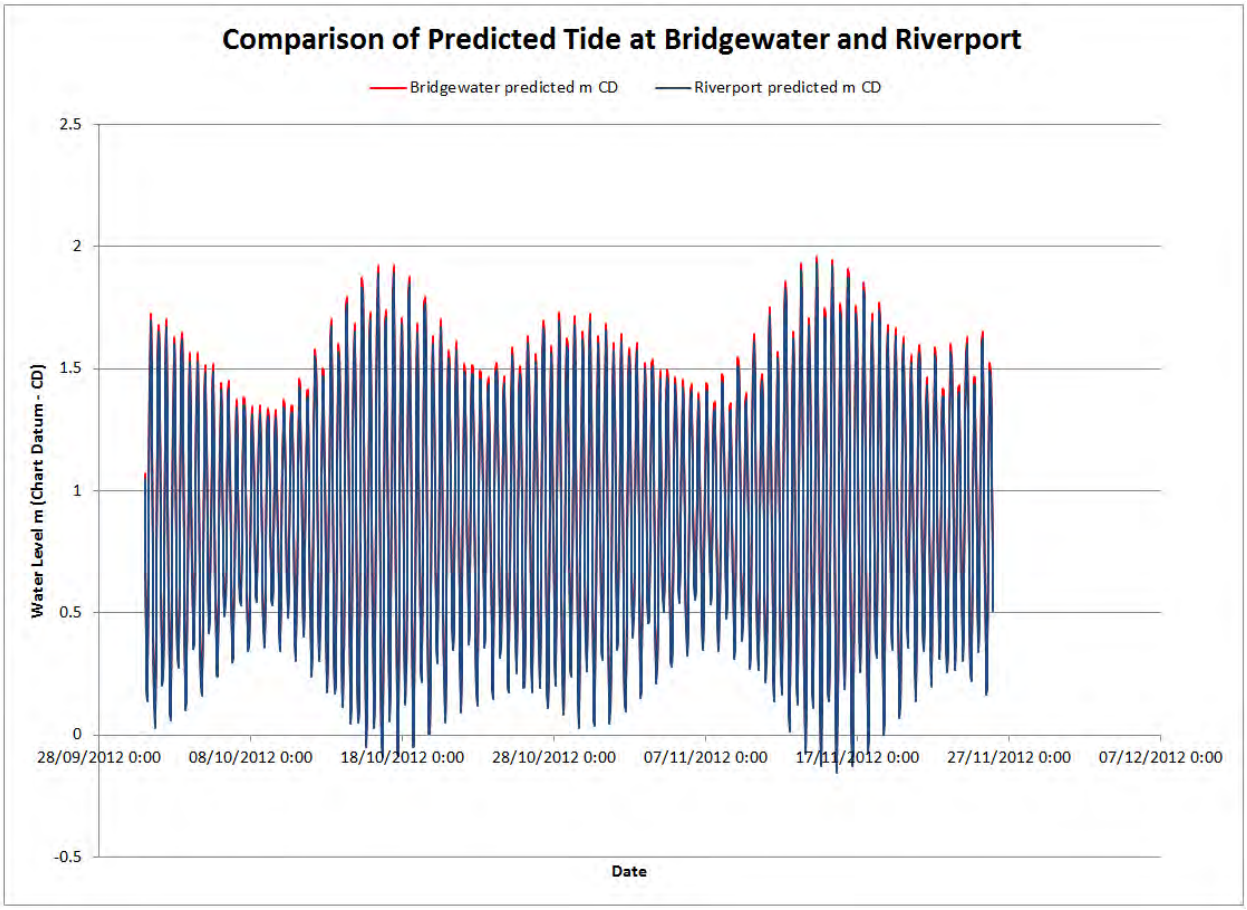

Figure 3:4 Comparison of predicted tide between Bridgewater and Riverport, relative to chart datum.

The data from the pressure sensors that were deployed in the water had to be compensated for variations in barometric pressure to ensure accurate readings. Reference points were defined along the wharf at each site and survey grade GPS measurements were obtained for the elevation, and converted to CGVD28, and used to convert the tidal elevations relative to this datum so it can be related to the lidar DEM and other topographic data. The observed water levels obtained at Kraut Point and Bridgewater (Marine Terminal) are consistent with the predictions in that the water level is higher at Bridgewater than Kraut Point (Figure 3:5).

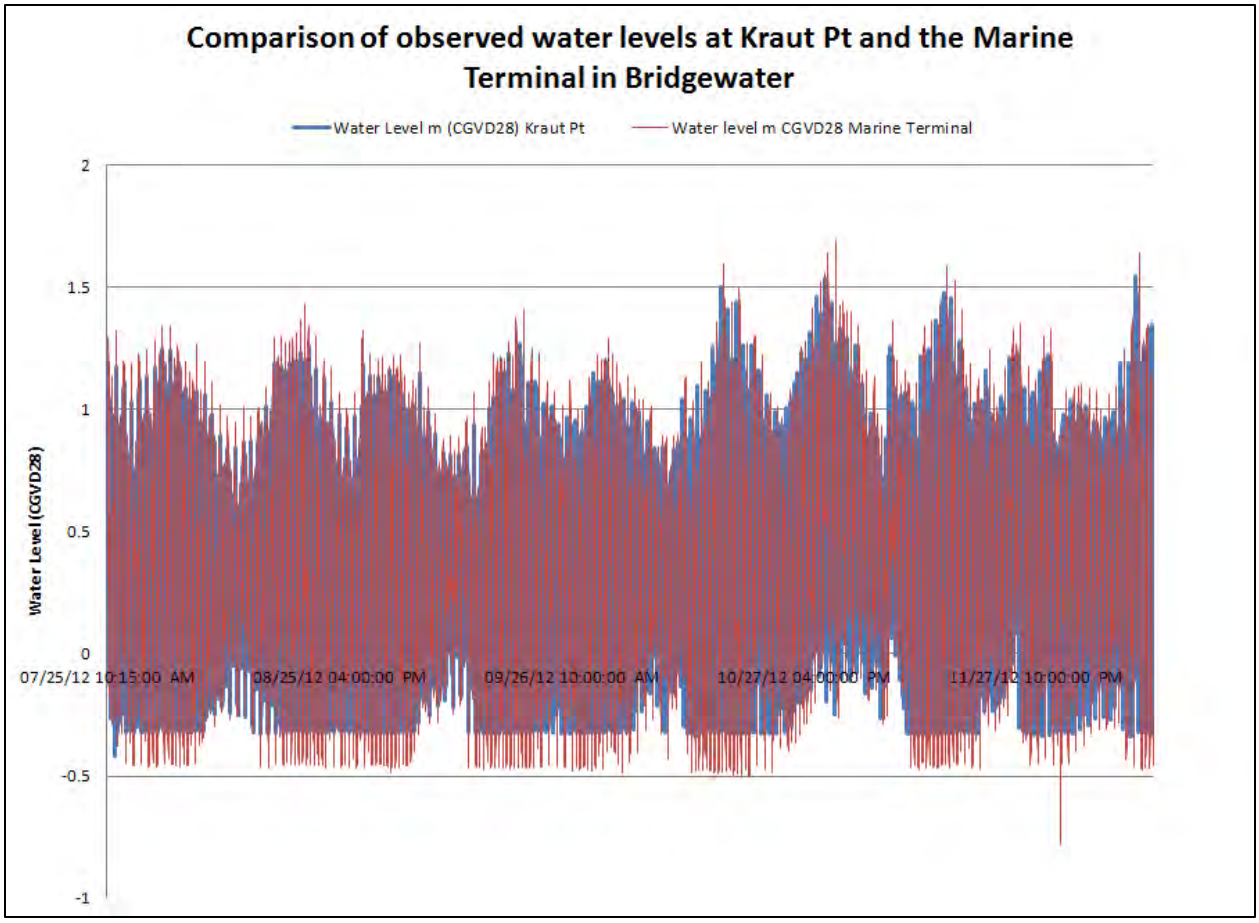

Figure 3:5 Comparison of observed water levels from Kraut Point and Bridgewater July-Dec. 2012.

Both sites experienced storm surges in November and early December. The predicted tide was integrated and adjusted from chart datum to CGVD28 and the residuals were calculated to show storm surge levels. This was achieved by subtracting the observed water level from the predicted water level (Figure 3:6). The largest storm surges recorded during this period were on the order of 50 to 70 cm, producing total water levels ranging from 1.5 and 2 m (CGVD28) depending on the tidal height at the time of the surge. The Halifax tide gauge operated by CHS was downloaded and similar surges were observed in that observational record using a similar technique of comparing the observed and predicted tide.

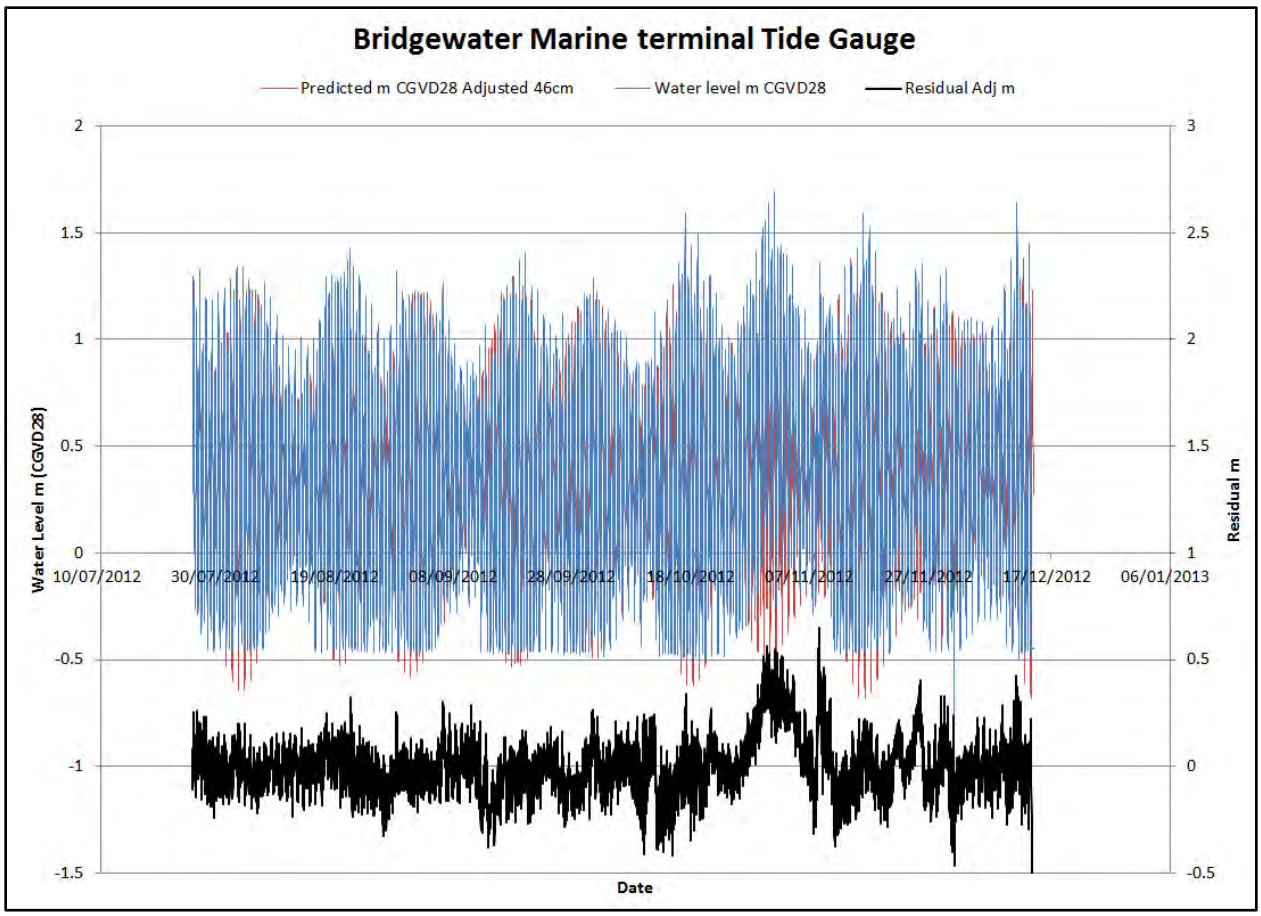

Figure 3:6 Observed and predicted water level for Bridgewater and storm surge residuals.

3.2. Lidar Terrain Model

The lidar data were validated and a DEM and DSM surface model constructed. The bathymetry and river cross-section information were interpolated along with the lidar surface models to construct a seamless elevation model that represents the topography above and below the water line. This bathymetry grid was then resampled to different resolutions to be used in the modeling procedure. The lidar surface models were also used to evaluate how well buildings could be extracted from the DSM. The flood inundation models were then intersected with the lidar models to construct the flood risk maps. In addition to the raw lidar surface model grids, colour shaded relief models were constructed from the DSM and DEM for enhanced interpretation and visualization of the terrain (Figure 3:7).

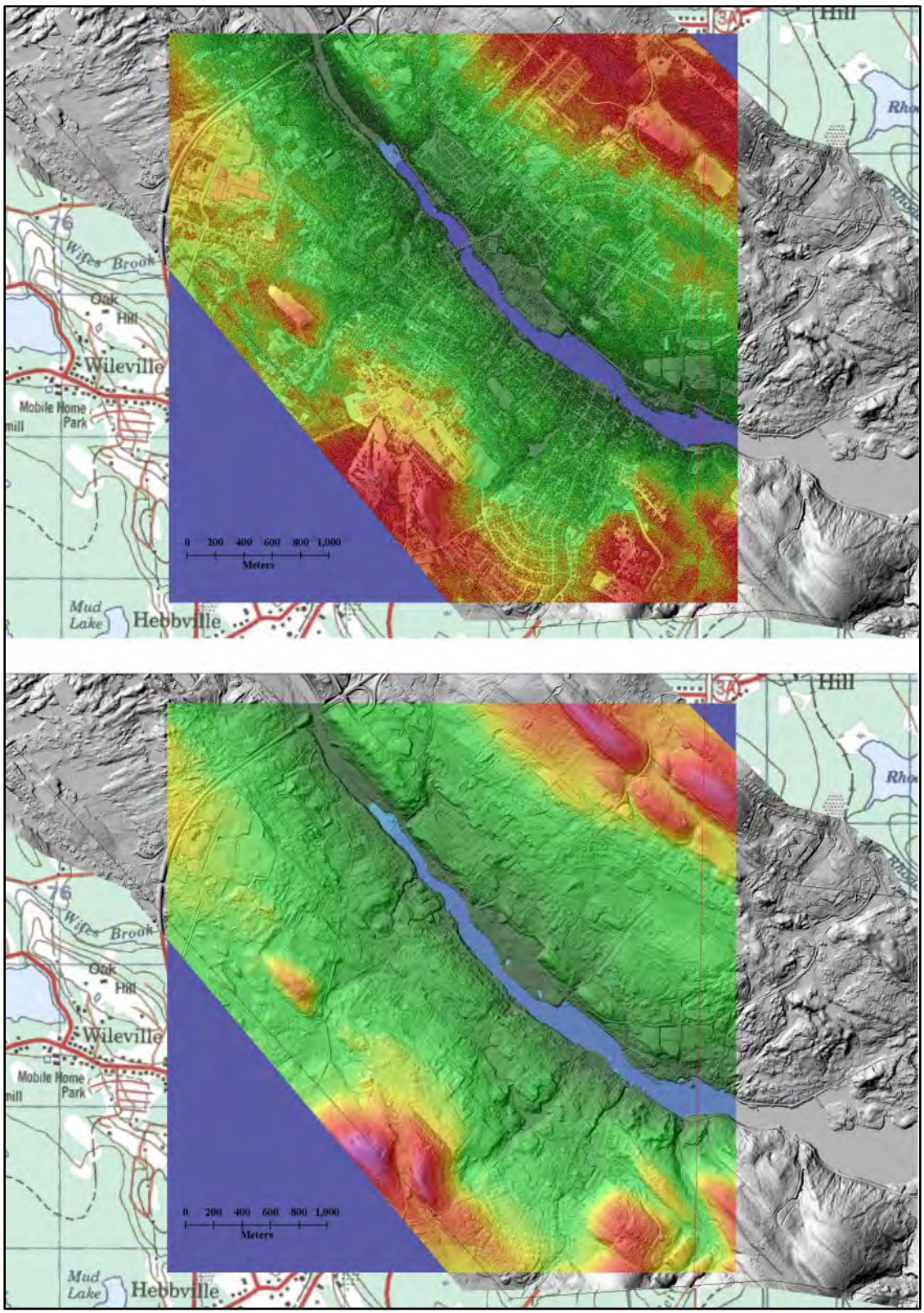

Figure 3:7 Example of close up colour shaded relief models for the DSM (top) and DEM (bottom) for the Town of Bridgewater.

3.3. Hydrologic modeling

As described earlier, a river runoff model was initially constructed for the LaHave watershed with the intention of driving the river discharge component of the model. The rainfall and temperature record from Kejimkujik (Keji) Environment Canada weather station for 2010 was used to estimate regional hydrology parameters by considering factors such as soil permeability and land cover. The initial validation of this model was done by comparing the modeled discharge and the observed discharge as measured by the Environment Canada gauge upstream of Bridgewater (Figure 3:8). Areas of disagreement can be explained by the fact that rainfall events in Keji may not have occurred in the LaHave watershed and vice versa.

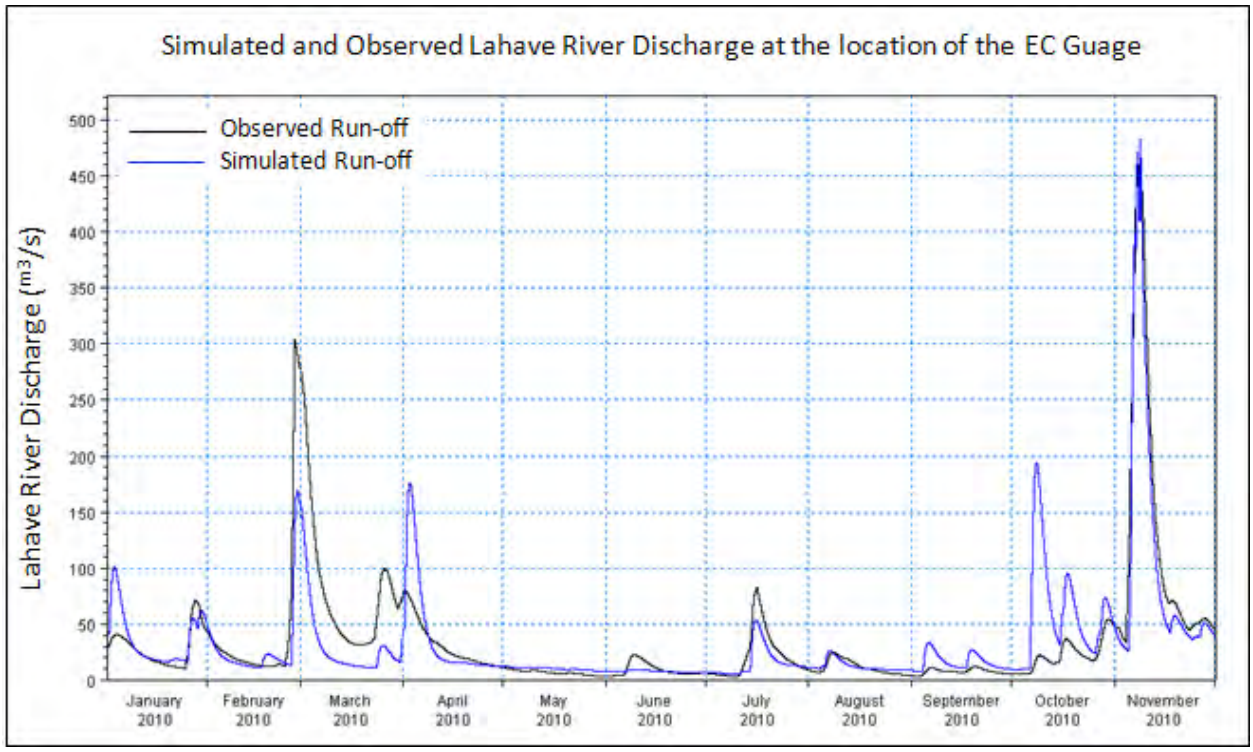

Figure 3:8 Comparison of the simulated and observed discharge of the LaHave River.

Due to the fact that there was no local long term weather station to drive the model and examine flooding events it was decided that the Environment Canada LaHave river discharge data series directly in the modeling.

The Kraut Point tide gauge was used to validate the tidal boundary condition that was used for the Mike 21 component of the modeling for the week of July 25, 2012 (Figure 3:9)

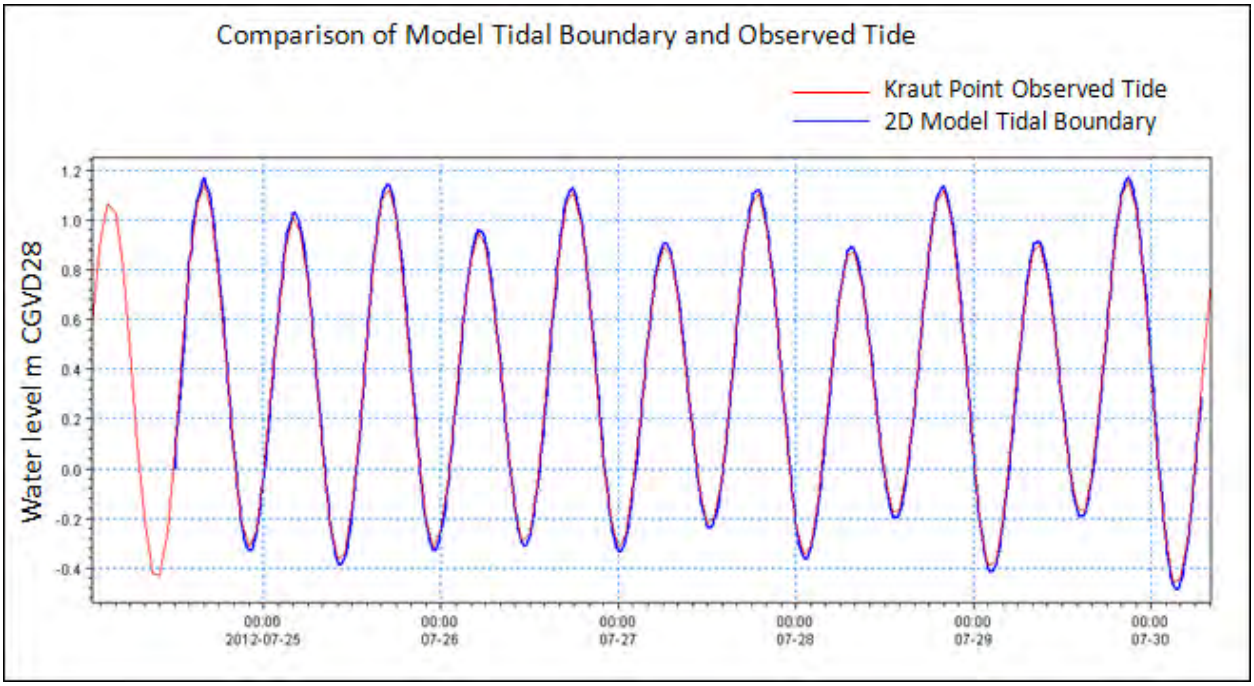

Figure 3:9 Mike 21 tidal boundary (blue) comparison of the observed water level at Kraut Point (red).

The various modeling scenarios constructed can be separated into three types: 1) river flooding alone based on discharge, 2) storm surge flooding alone from the ocean, and 3) combined discharge and storm surge flooding.

Two styles of models have been used to date on this project. The Mike-11 model is used for river flooding and is a 1-dimensional model that is based on cross-sections of the river and floodplain. The other type of model is a 2-dimensional model known as Mike-21, which is typically used for ocean and near shore circulation and tidal modeling. The two models can be interfaced to produce a Mike Flood model which is a 2-D model that combines the discharge from Mike-11 with the ocean levels from Mike-21 and calculates the areas to be inundated based on the 2-D topography.

We have produced results using both methods. The 2-D Mike Flood method was used for the 3 m nested grid for the LaHave River discharge and storm surge simulations. The Mike-11 watershed cross-section based method was used to map the flood extent for the two streams that flow northeastward through the town and are prone to flooding. The 2-D Mike Flood model that combined river discharge with the tidal and storm surge values was validated using the AGRG tide gauge at the Marine Terminal and at Kraut Point. In both cases where the tide gauge water level observations (Kraut Point and the Marine Terminal) are compared to the model results, the model does not account for atmospheric forcing issues that could affect the water level such as wind and variations in atmospheric pressure. However, the

validation results of the model indicate that over a four day period (Oct. 23-27, 2012) the mean difference in observed and modeled water levels at Kraut Point (27 m grid domain) is -2.8 cm with a standard deviation of 7.1 cm and the mean difference in observed and modeled water levels at the Marine Terminal (3 m grid domain) is 7.1 cm with a standard deviation of 20.1 cm (Figure 3:10). The increased noise in the water level observations at the Marine Terminal are interpreted to be a result of the finer grid cell size and the combined effects of river discharge and tide and the location of the gauge compared to the location where the model values were extracted. However, the results of the validation of the model are within the range of the absolute vertical accuracy of the lidar data (15-30 cm) and thus suitable for lidar based flood mapping. The specific location chosen for the marine terminal tide gauge, being the shore side of the marine terminal wharf, may have further contributed to the apparent noise in both the gauged (red line) and modeled (blue line) water levels due to micro-tidal effects between the wharf and the shore and a lack of near shore bathymetry for that area (Figure 3:10).

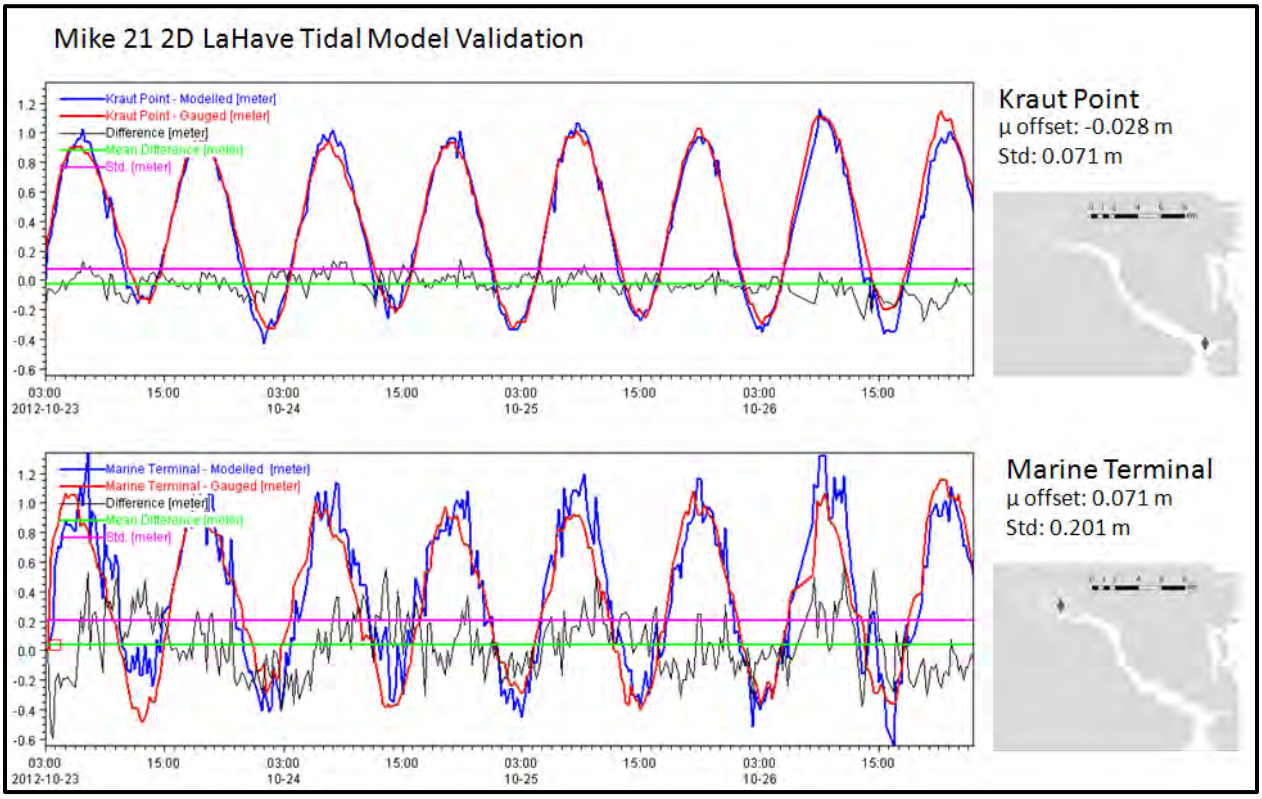

Figure 3:10 Model validation results. Comparison of tide gauge observations with model results for the 27 m grid at Kraut Point (top) and the 3 m grid at the Marine Terminal (bottom).

The 1-D cross-section Mike-11 model results for the streams were validated based on the photographic evidence supplied.

As mentioned, the model for the LaHave River estuary consisted of a 1-D and a 2-D model. The 1-D model extends from the Environment Canada Gauge located upstream of the town to the estimated extent of the tidal influence of the river, which is between the Highway #103 bridge and Veteran's Memorial Bridge. The 2-D model extends from the downstream 1-D boundary to the mouth of the LaHave River. The output from the 2-D model simulations are limited to this area and extend just beyond the town limits. The output from the 1-D river model extends from the upstream extent of the 2-D model to just beyond the town boundary. The two streams within the town that were modeled in 1-D are limited to just beyond the town boundary and the LaHave River. In simpler terms, the flood extents are delivered in three sets of files: 1) the main LaHave River for the downtown waterfront; 2) LaHave River upstream of the tidal influence (between the Highway #103 bridge and Veteran's Memorial Bridge); and 3) the two streams within the town. The three flood layers have been combined for presentation in the following figures (Figure 3:11-Figure 3:15). The flood risk map of the LaHave River (1-D and 2-D results) for the 50 year discharge event at a 99.5% probability under normal high tide conditions is presented in Figure 3:11. If we take the same 50 year return period and reduce the probability of occurrence to 65%, which is equal to at least 1 occurrence within 50 years, the increased discharge has an effect of overtopping the river channel upstream of the Memorial Bridge Figure 3:12. In Figure 3:11 and Figure 3:12 there is minimal flooding adjacent the LaHave River in the main part of the town where the channel is deeper and there is a tidal influence. All of the various flood risk maps from the simulations are presented in Appendix 5.

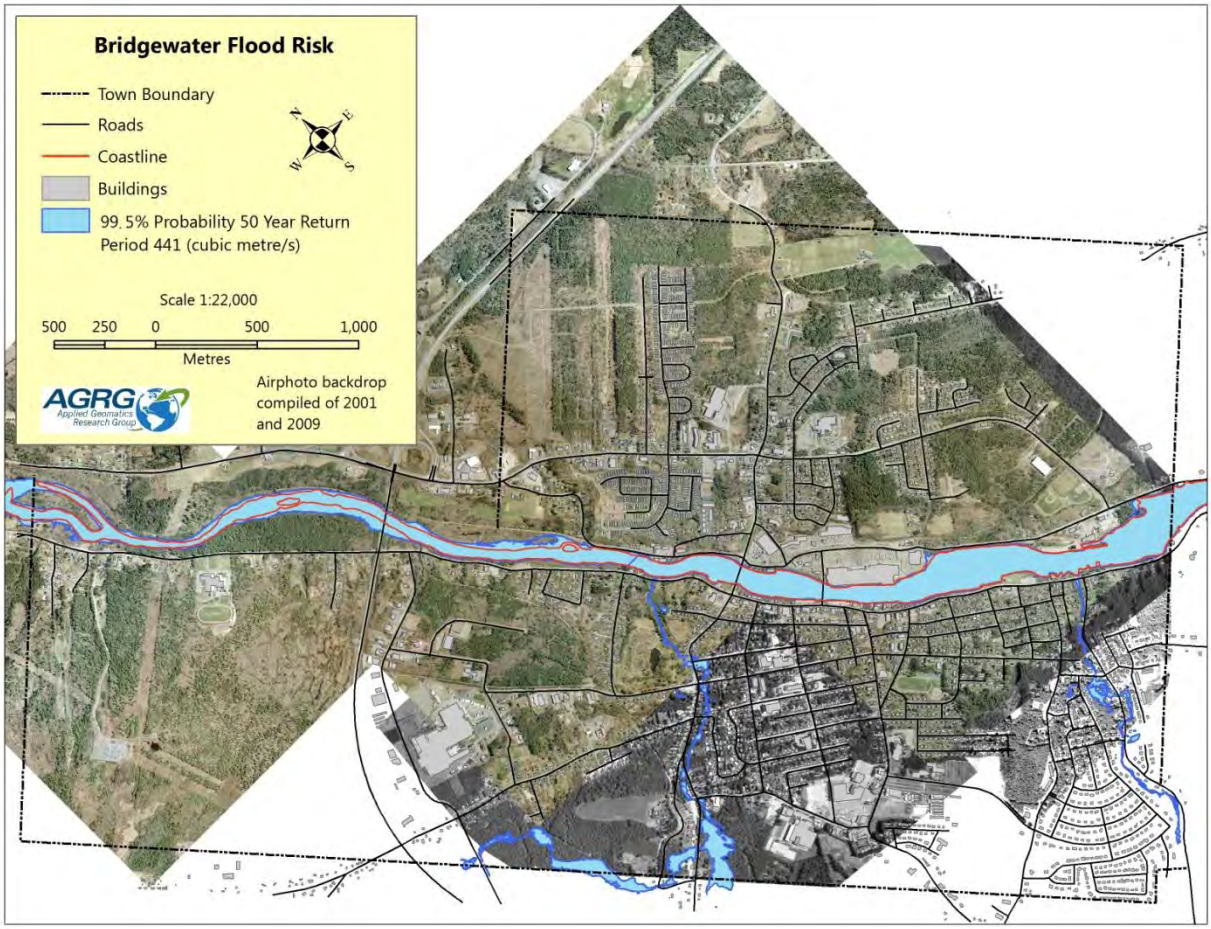

Figure 3:11 Flood risk map for the **99.5%** probability of occurrence for the **50 year** return period discharge with **normal** high tide.

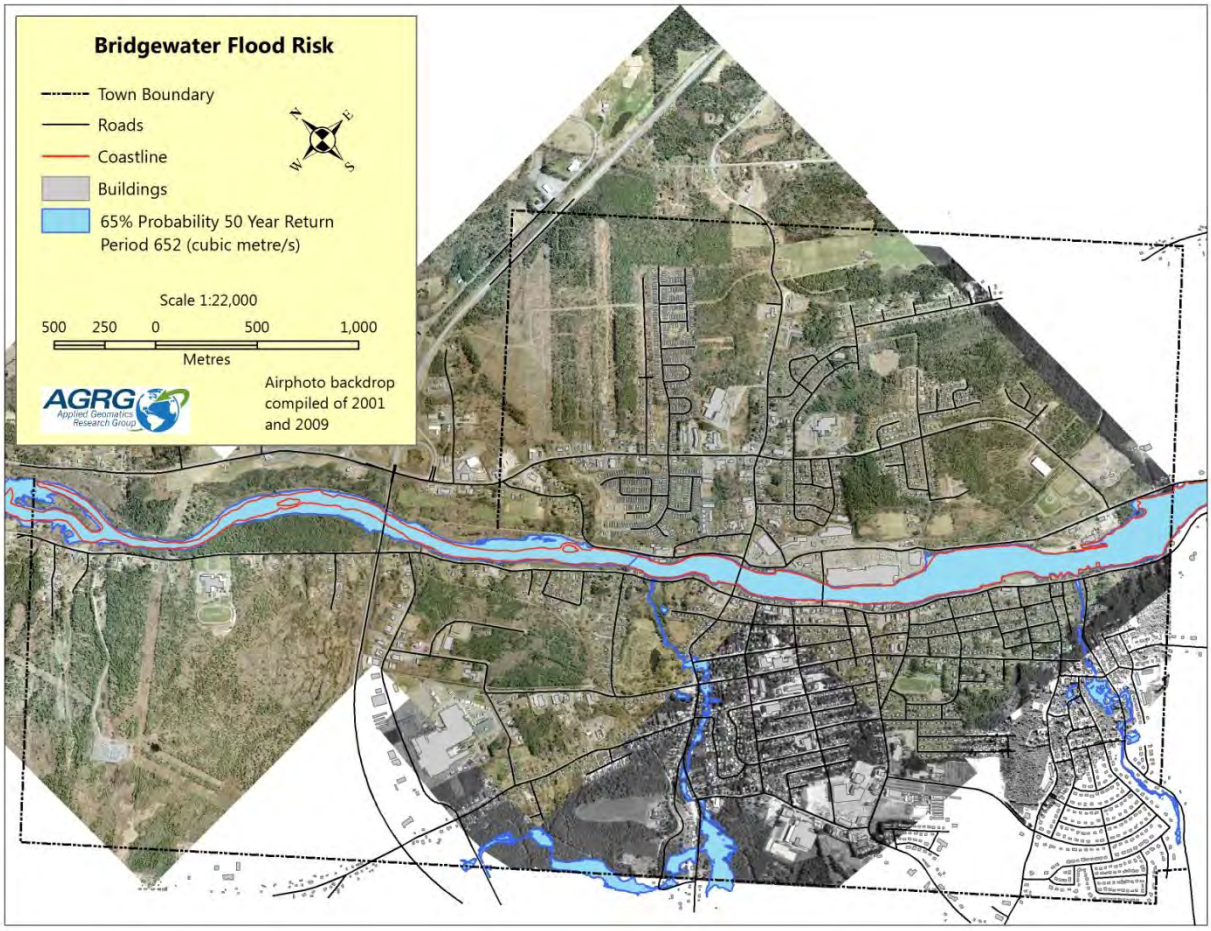

Figure 3:12 Flood risk map for the **65%** probability of occurrence for the **50 year** return period discharge with **normal** high tide.

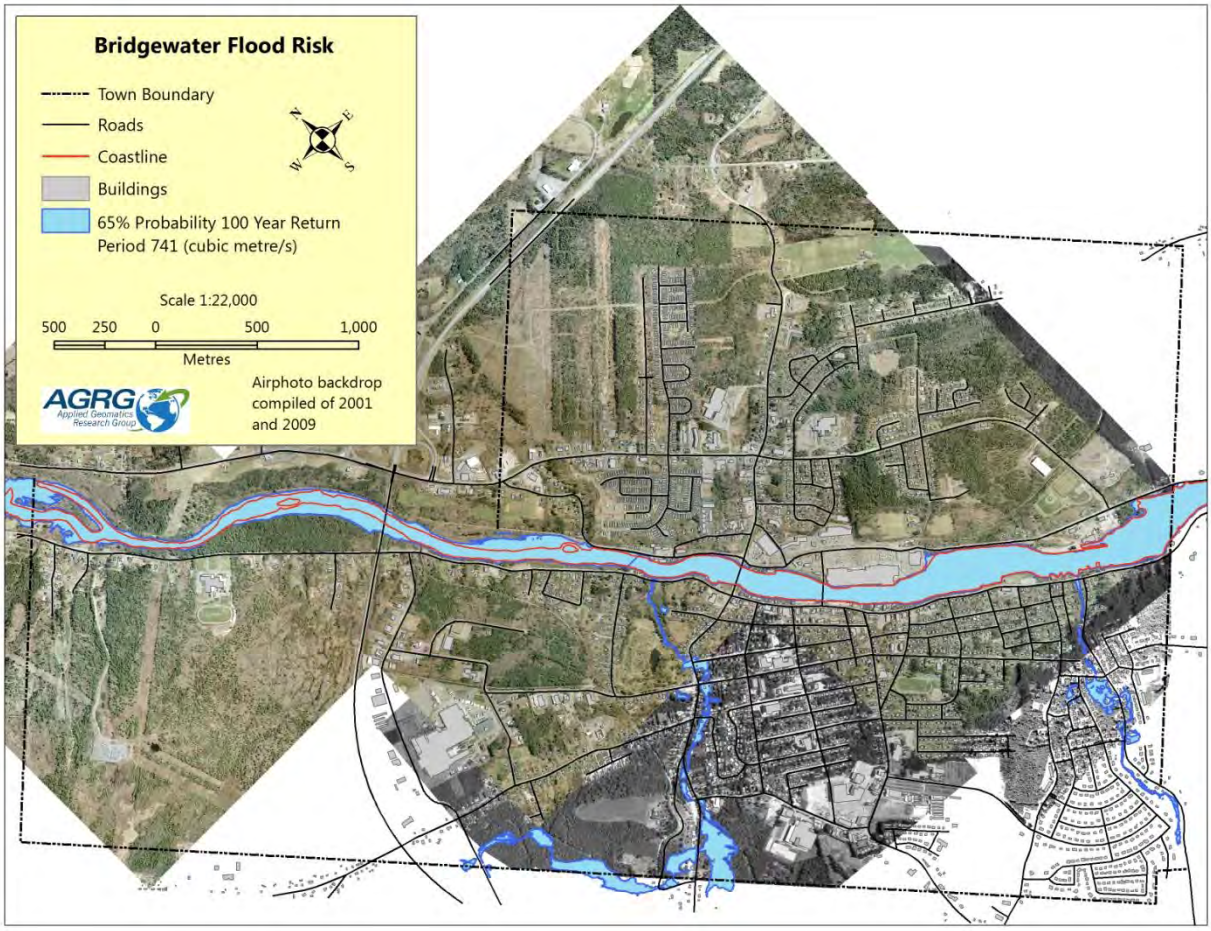

Figure 3:13 Flood risk map for the **65%** probability of occurrence for the **100 year** return period discharge with **normal** high tide.

If we examine the 100 year return period of discharge at the 65% probability, flooding upstream of the town expands slightly (Figure 3:13). However when we simulate the same 100 year return period discharge at a 65% probability with a 2.2 m storm surge at the mouth of the LaHave River boundary, sections of the town adjacent to the river get inundated (Figure 3:14). The parking lot surrounding the Bridgewater Mall floods, the Marine Terminal Wharf is overtopped along with flooding of Shipyards Landing Park along the waterfront. LaHave Street and Route 3 flood southeast of the Marine Terminal as well as LaHave Street upstream of the Veteran's Memorial Bridge.

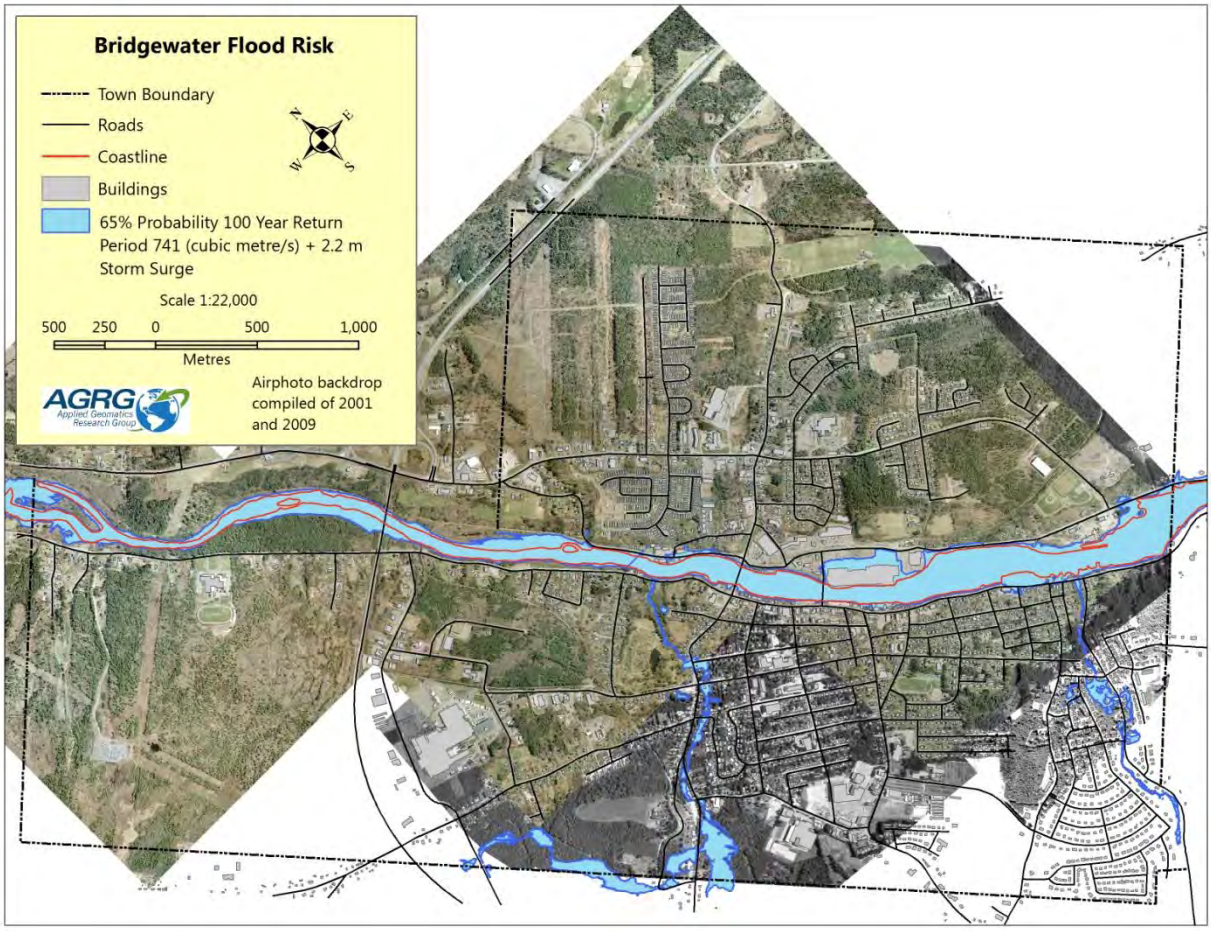

Figure 3:14 Flood risk map for the **65%** probability of occurrence for the **100 year** return period discharge with a **2.2 m** storm surge during a normal high tide.

However, when we simulate the same 100 year return period discharge at a 65% probability with a 3.5 m storm surge at the mouth of the LaHave River boundary even more sections of the town adjacent to the river get inundated (Figure 3:15). The flood extends beyond the parking lot of the Bridgewater Mall and up to LaHave Street, and inundates Old Bridge Street and Davison Drive. The flooding extends from overtopping the Marine Terminal Wharf to inundating LaHave Street and Route 3 either side of the terminal. Flooding expands to cover a larger section of LaHave Street upstream of the Veteran's Memorial Bridge including lower Elm Street. Flooding at Shipyards Landing Park along the waterfront expands to cross King Street and the lower section of School Street. The area surrounding the southwest side of Veteran's Memorial Bridge begins to flood also (Figure 3:15).

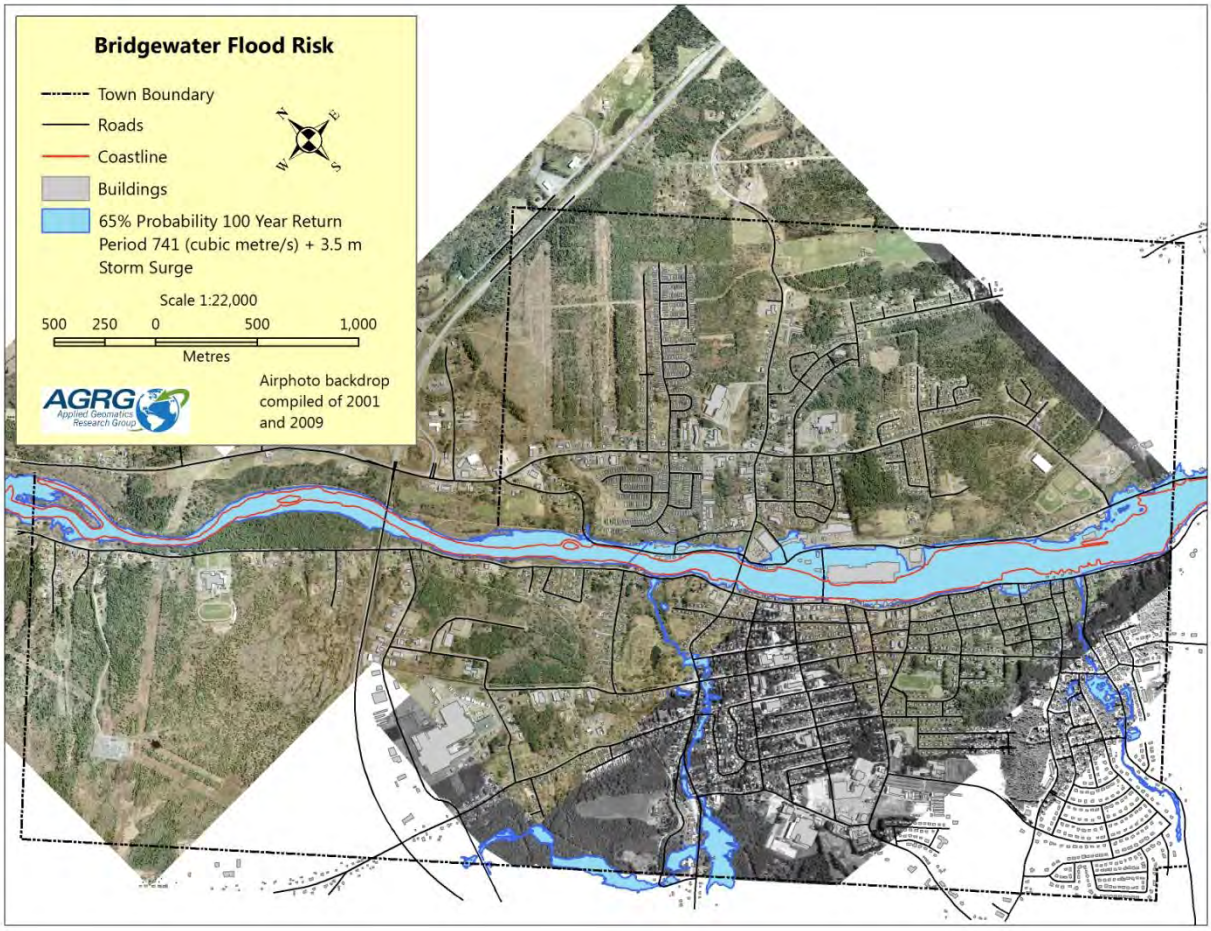

Figure 3:15 Flood risk map for the **65%** probability of occurrence for the **100 year** return period discharge with a **3.5 m** storm surge during a normal high tide.

These simulations and maps demonstrate that the main downtown area along the waterfront are much more susceptible to storm surge and long term sea-level rise than to increased discharge of runoff from the LaHave watershed.

However, the streams-brooks that drain northeast through the town into the LaHave River are sensitive to rainfall runoff events, but not storm surge. Wile Brook appears to have the worst flooding problems based on discussions with town officials and photographic evidence. Flooding also occurs on Stewart Brook and Hebb Brook. Based on the storm sewer maps provided by the town, the surface drainage area is not representative of the water distributed to Stewart Brook and we could not accurately model this system. However we did generate flood risk maps for Wile Brook and Hebb Brook (Figure 3:16). The scaled and amplified by three times the 50 year return period discharge at a 99.5% probability floods sections of both brooks (Figure 3:16).

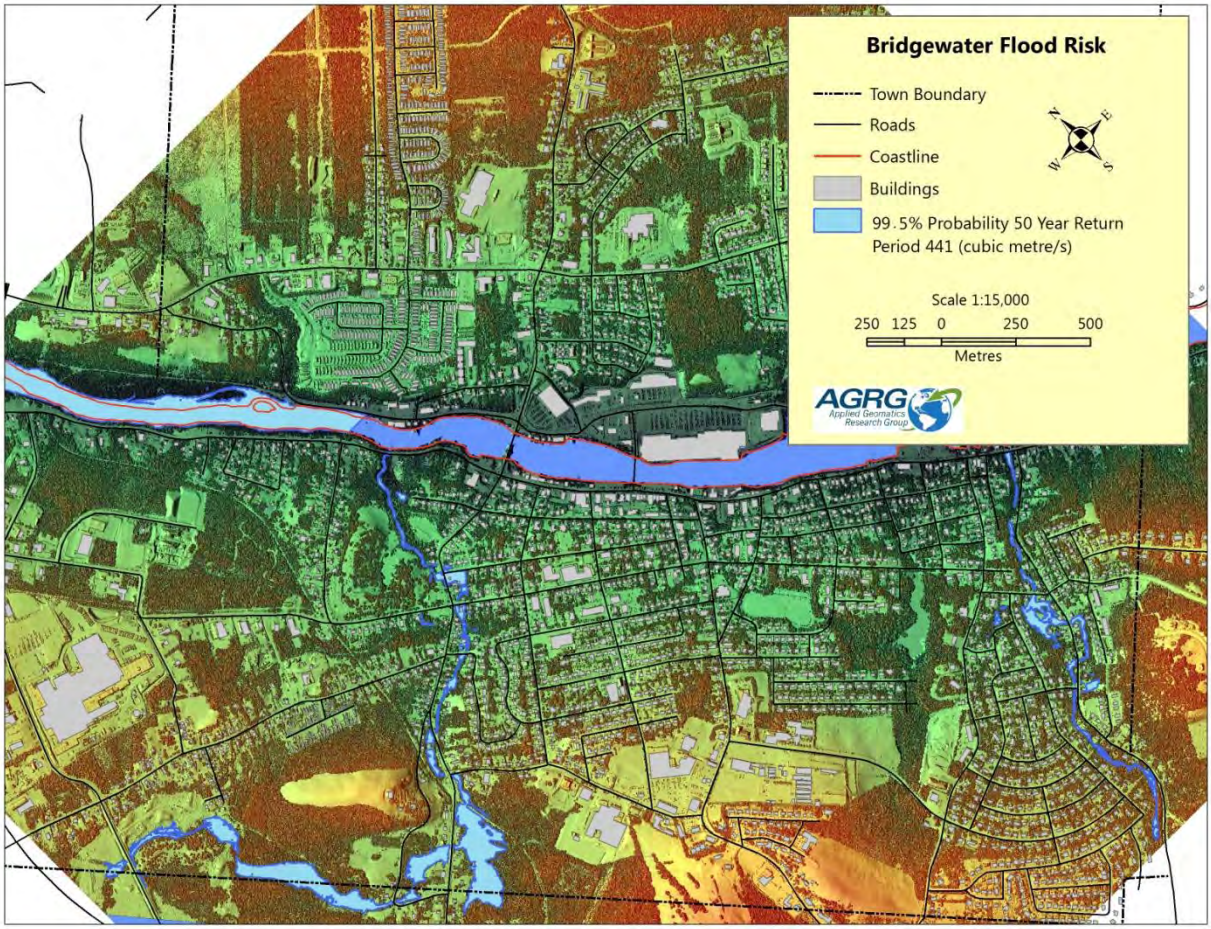

Figure 3:16 Flood risk map for the **99.5%** probability of occurrence for the **50 year** return period discharge event with **normal** high tide. The flood extent in blue is plotted over the lidar colour shaded relief Digital Surface Model (DSM) for Wile Brook (left) and Hebb Brook (right).

The scaled and amplified by three times the 50 year return period discharge at a 65% probability floods sections of both brooks (Figure 3:17).

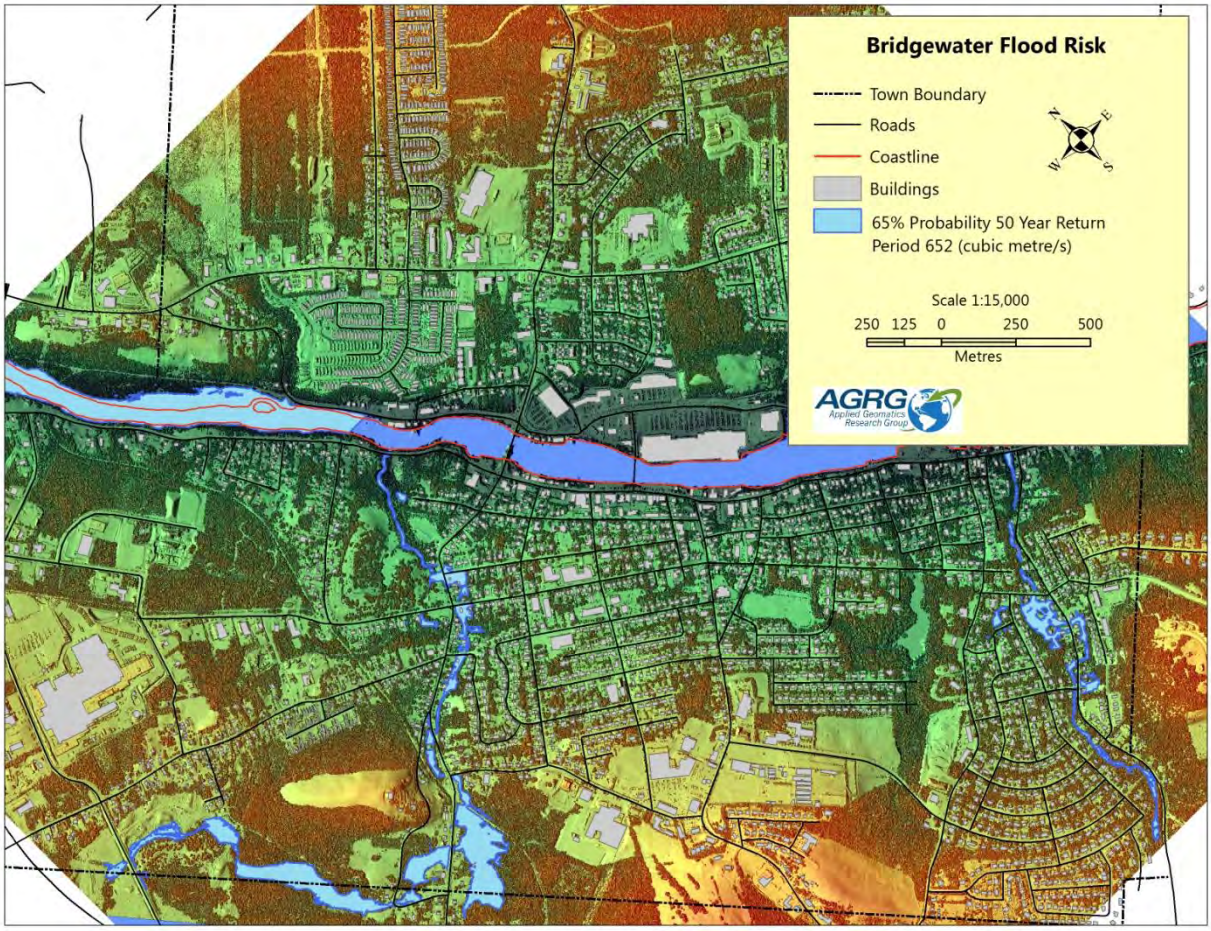

Figure 3:17 Flood risk map for the **65%** probability of occurrence for the **50 year** return period discharge event with **normal** high tide. The flood extent in blue is plotted over the lidar colour shaded relief Digital Surface Model (DSM) for Wile Brook (left) and Hebb Brook (right).

3.4. River Bank Erosion

The study area included the east and west banks of the LaHave River 1-2 kms on either side of Bridgewater, NS (Figure 3:18). There are varying degrees of slope along the shoreline in the study area, ranging from shallow (<10°) mud flats near the mouth of the harbour, to intermediate slopes (10° - 30°) along most of the river bank, to steep (>30°) shoreline topped with roads and other infrastructure (Figure 3:19).

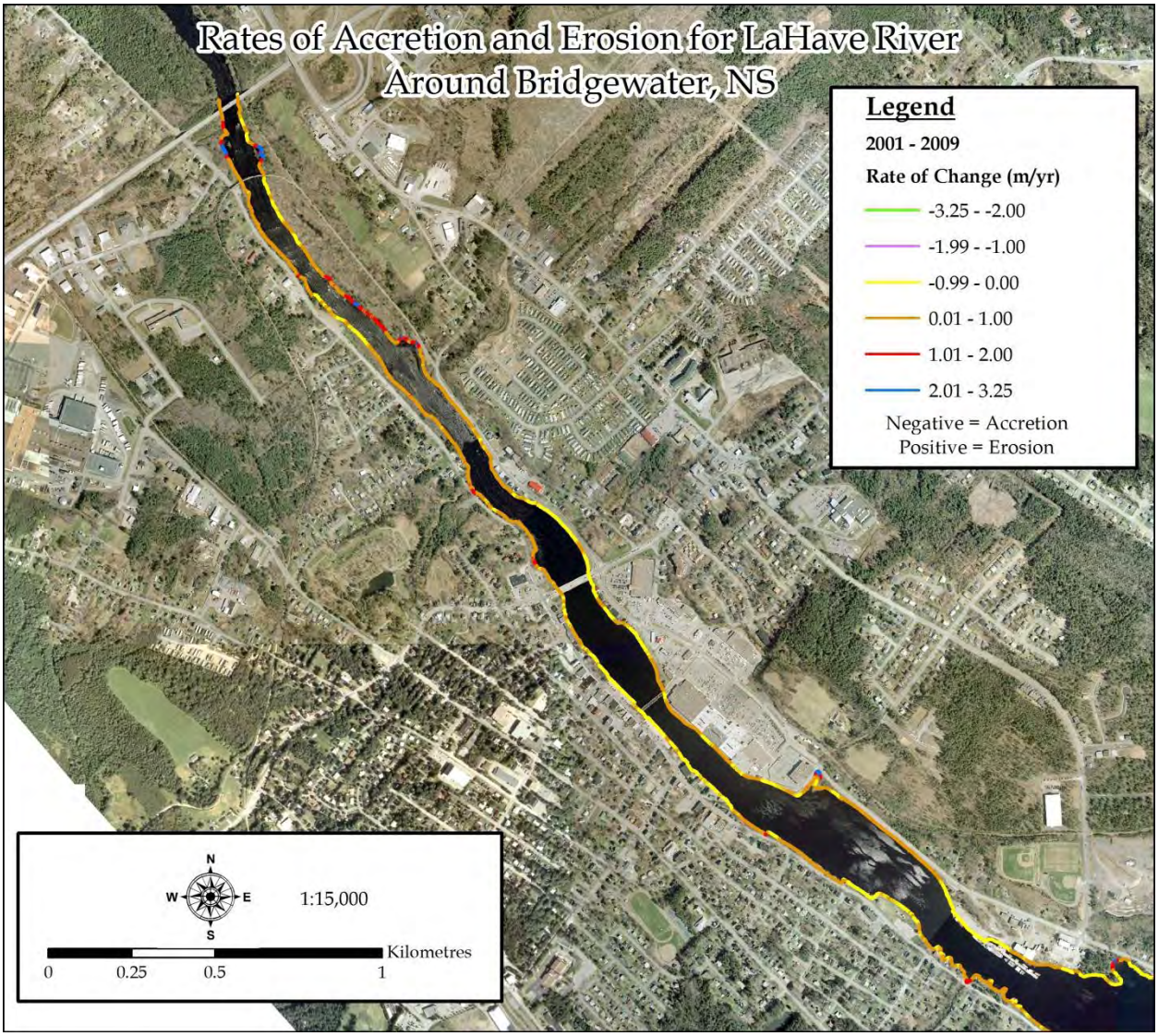

Figure 3:18 Overall study area showing rates of change (in metres per year) of accretion and erosion from 2001-2009 for the LaHave River. Negative values indicate accretion. Imagery shown is from 2001 and 2009.

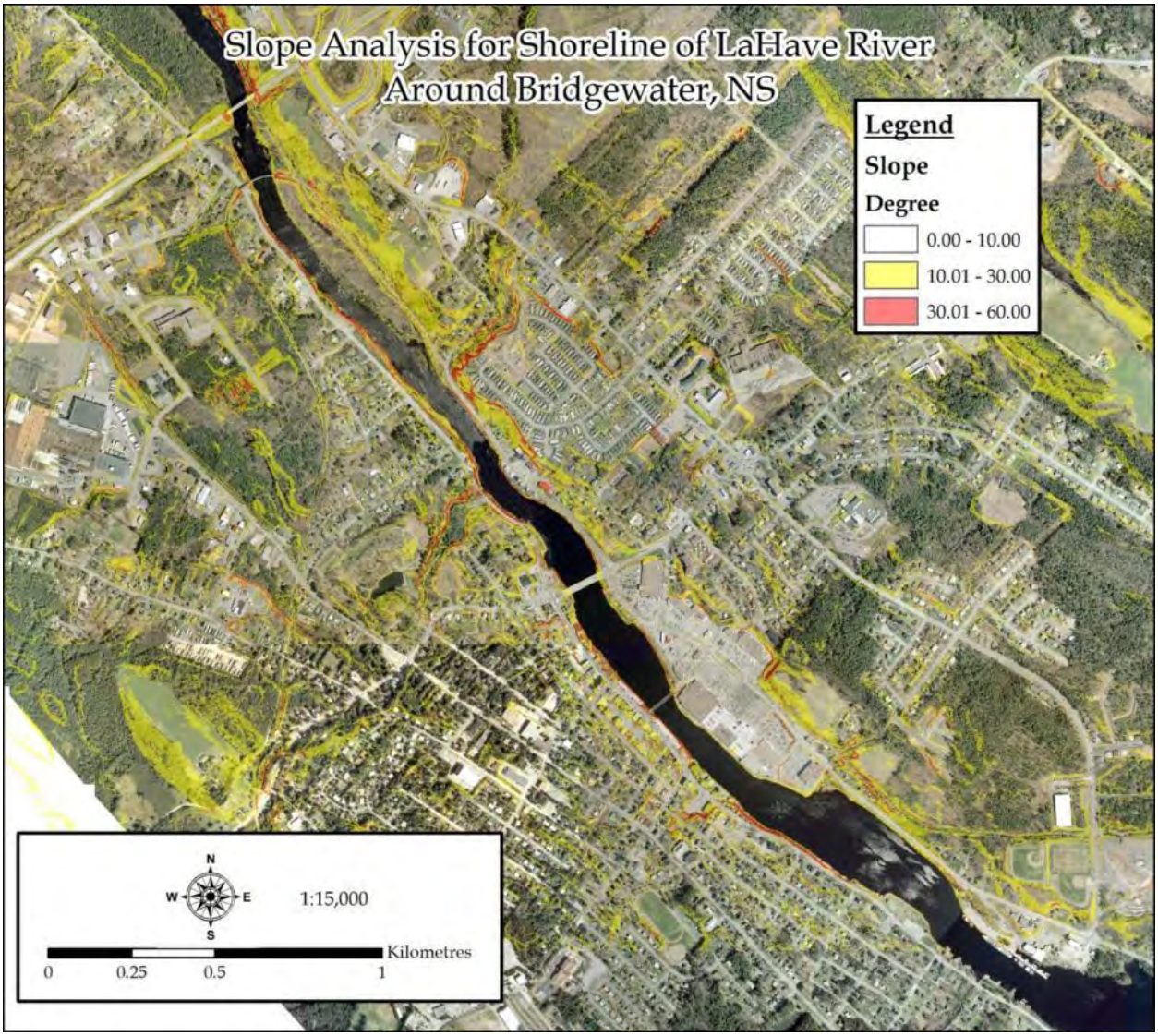

Figure 3:19 Slope analysis showing slopes of between 30°-60° (red), 10°-30° (yellow) and 0°-10° (no colour). Imagery taken in 2001 and 2009.

Although islands were initially delineated no islands in the river were assessed for accretion or erosion in this study.

The shoreline vectors for each year were compared with shoreline delineated from the most recent 2009 dataset. The distance (in metres) between the 2009 and target year's shorelines were calculated. These distances were then divided by the number of years over which they occurred, and the results were shown as a rate of change in metres per year.

The rates of change for each temporal comparison were analyzed to find the maximum rates of change for both erosion and accumulation, as well as the means and their standard deviations. The rates were

analyzed yearly as a whole (Table 3-1) as well as broken up into different areas (eg. east versus west river bank).

Table 3-1 The minimum, maximum, and mean rate of change (in m/yr) and standard deviations for each temporal comparison to the 2009 shoreline. Negative values indicate accretion.

Year	Max Rate of Accretion	Max Rate of Erosion	Mean	Std. Deviation
1948_2009	-0.82	0.55	0.00	0.12
1965_2009	-0.75	0.75	0.00	0.14
1967_2009	-0.79	0.78	0.00	0.15
1992_2009	-0.88	1.59	0.12	0.23
2001_2009	-1.40	3.25	0.33	0.55

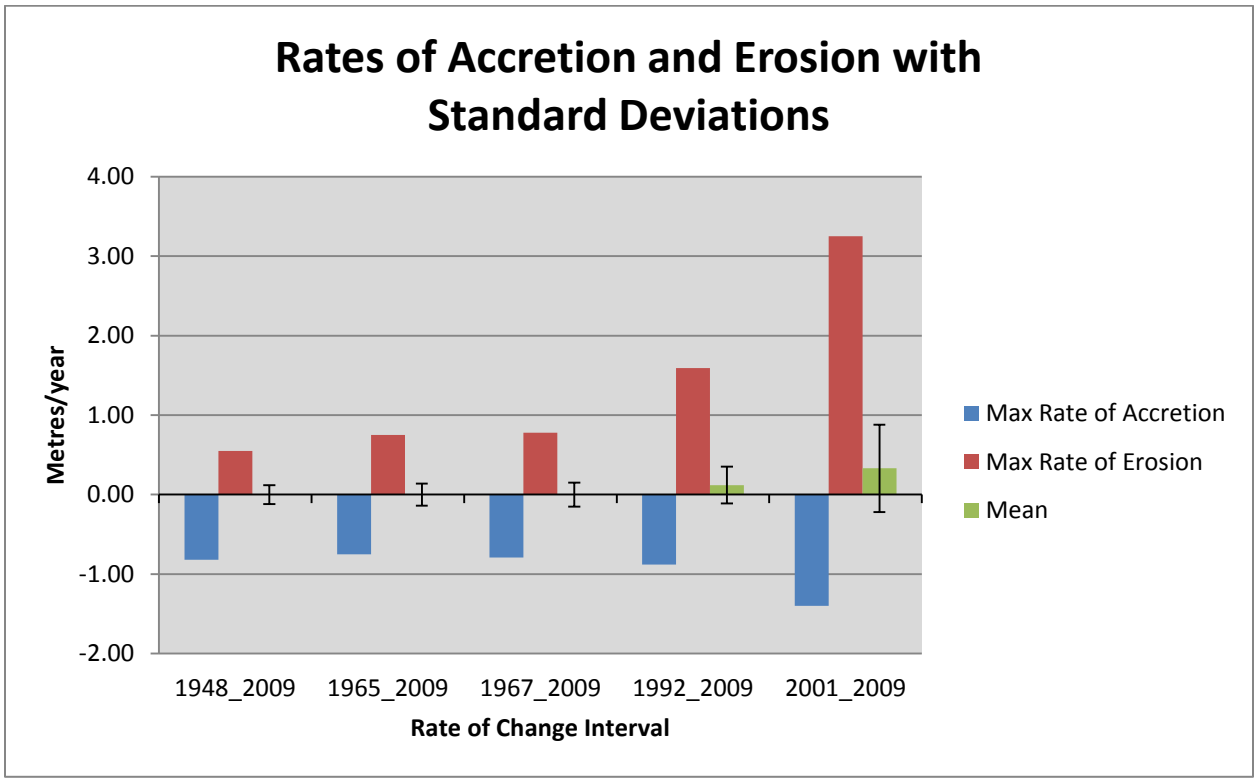

Figure 3:20 A graph showing the rates of accretion (positive values) and erosion (negative values), along with the mean and standard deviations, for all five time frames analyzed.

The highest mean rate of change was found in the comparison of the 2001 to 2009 dataset. The overall mean rate of change was 0.33, indicating overall erosion at a rate of 0.33 m/yr. The increasing standard deviation throughout the temporal datasets indicates increasing variability of erosion and accretion events, such as severe precipitation or storm surges closer to the coast.

The highest rate of erosion change in the 2001 – 2009 dataset was found upstream from Bridgewater (Figure 6), where a rate of erosion exceeding 2.0 metres per year is seen on both east and west banks of the river. The highest rate of accretion change was found southeast of the Bridgewater Mall, where the maximum rate of change was -1.4 m/yr. This change is directly caused by the construction of a dock and not due to natural accretion.

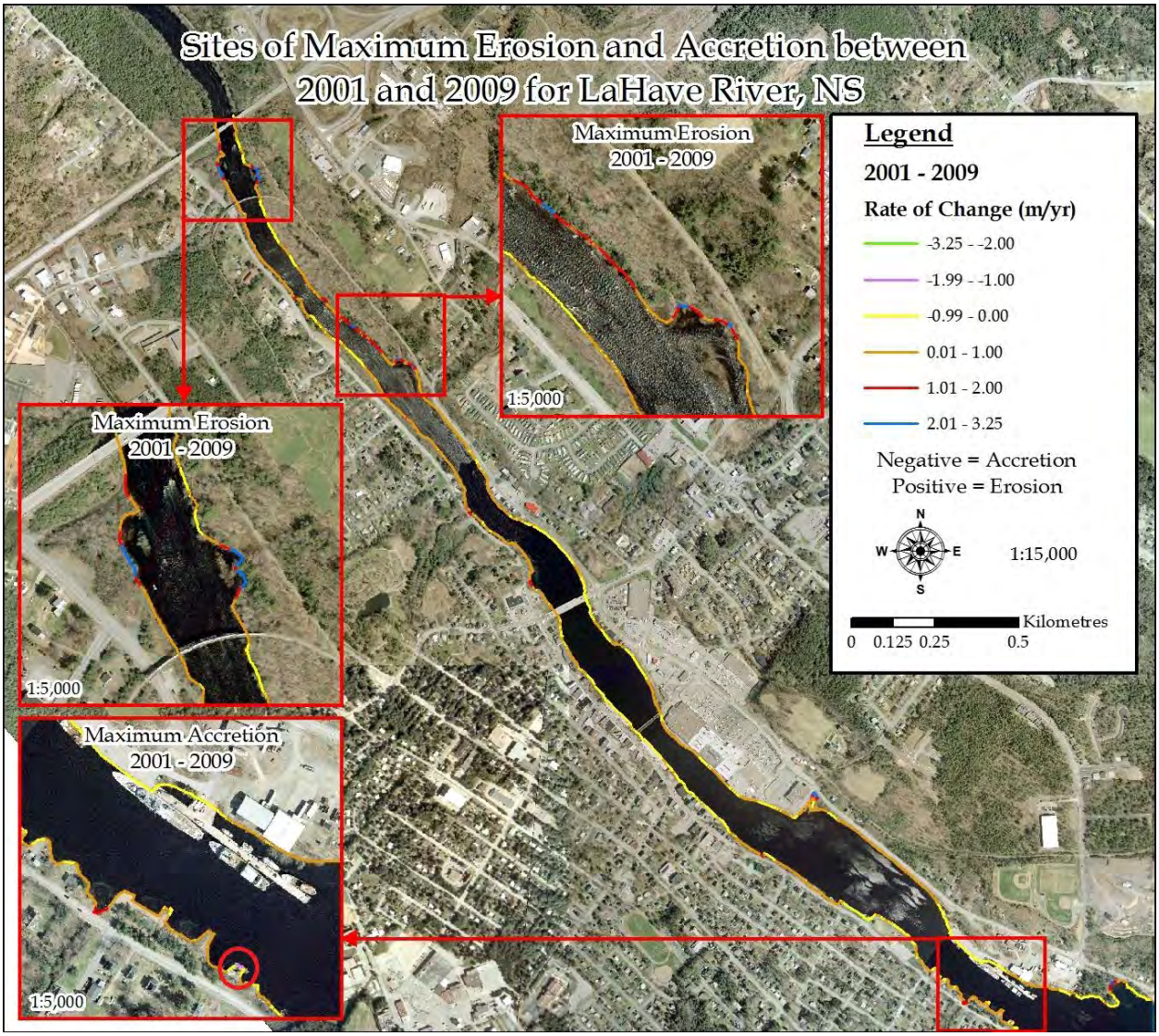

Figure 3:21 Areas with highest rates of change (positive and negative) from 2001-2009 for the LaHave River. Negative values indicate accretion. The imagery shown is from 2009.

The study area of the LaHave River was divided up into 5 roughly equal areas for further investigation (Figure 3:22). The mean rate of change

Table 3-2) was found for each year for each area, to show which areas accumulation/erosion are acting on the most. Area 4 including the Bridgewater Mall was found to be the area of highest rate of accretion throughout the years, particularly before 1967, which can be attributed to mass infilling along the east river bank to allow construction of the mall in the 1970's. Areas 1 and 2 showed the highest rates of erosion consistently through all time frames.

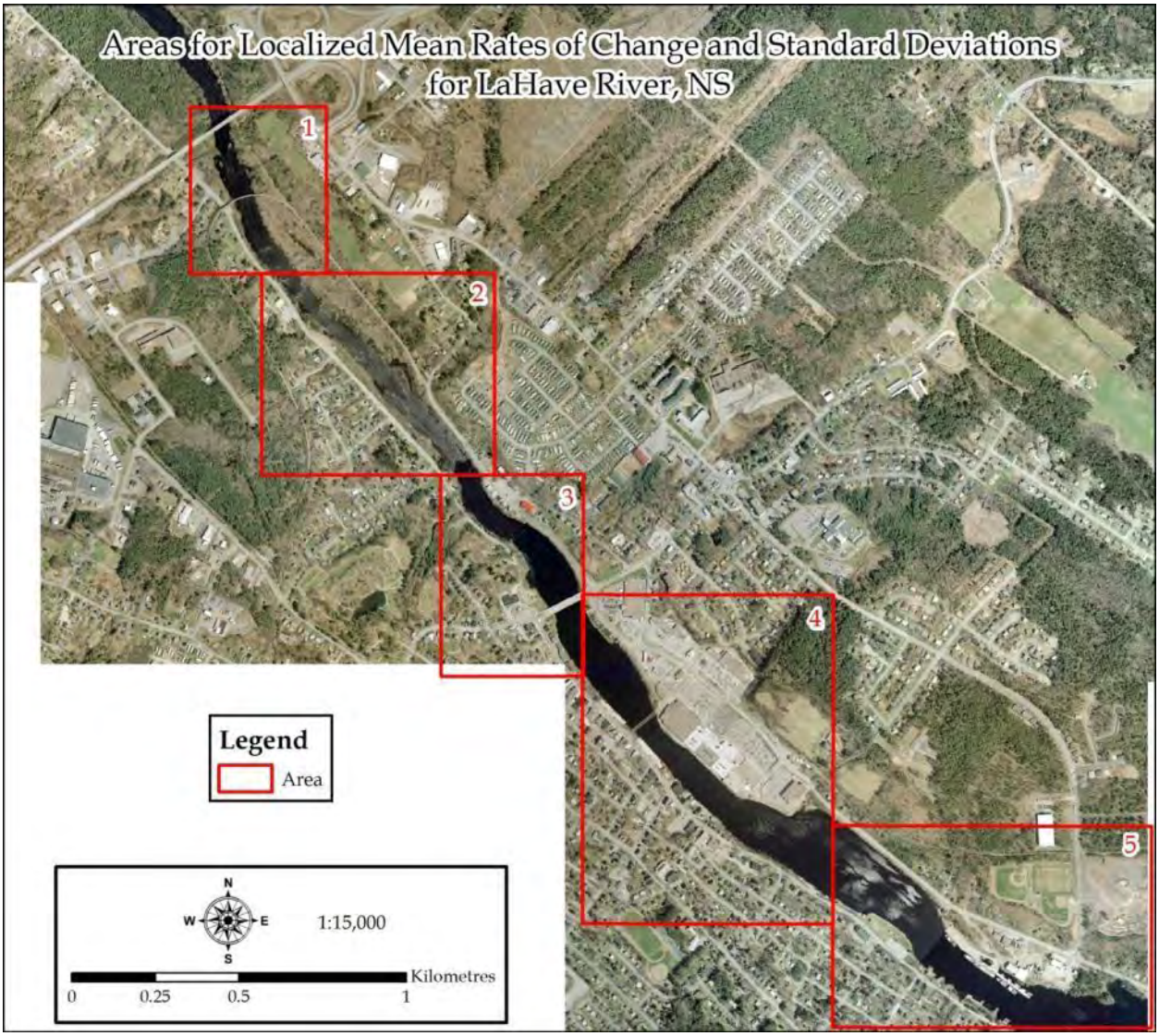

Figure 3:22 Areas used to determine localized mean rates of change. Imagery taken in 2009.

Table 3-2 Mean rates of change per area for each temporal dataset. Red values indicate the highest mean rate of erosion for that year while blue indicate highest mean rate of accretion for that year. Negative values indicate accretion.

Area	1948 - 2009	1965 - 2009	1967 - 2009	1992 - 2009	2001 - 2009
1	0.03	0.05	-	0.24	0.67
2	0.05	0.02	0.05	0.24	0.57
3	0.02	0.03	0.01	0.05	0.28
4	-0.08	-0.06	-0.07	0.10	0.13
5	0.00	0.04	0.00	0.01	0.18

Mean rates of change for each bank of the river were calculated to identify if one bank shows more accretion/erosion than the other. Overall, the mean rates of change for each bank were similar (0.10 m/yr loss on the east bank, 0.08 m/yr loss on the west bank) though a clear trend of increasing erosion on both banks of the river can be identified (Table 3-3).

Table 3-3 Mean rates of change by river bank for each temporal dataset (metres per year) for the LaHave.

	East Bank	West Bank
1948-2009	-0.01	0.01
1965-2009	0.00	0.02
1967-2009	-0.01	0.00
1992-2009	0.17	0.08
2001-2009	0.37	0.30
OVERALL MEAN	**0.10**	**0.08**

4. Discussion

The Town of Bridgewater is typical of many communities in Nova Scotia in that it is located on a major river that experiences the influence of the ocean and river runoff. This study has provided the opportunity to model the influence of tidal and river runoff components to flood risk along the LaHave River. The results of the analysis indicate that the main infrastructure of the town along the water front appears to be more vulnerable to flooding as a result of storm surge events and long-term sea-level rise than river runoff events. However, the areas adjacent to the LaHave River upstream of the Veteran's Memorial Bridge are more influenced by runoff events than downstream and may be susceptible to erosion during extreme river discharge events. At the present time there is very little development and infrastructure in this upstream area. The results of the coastline change detection analysis reveal a similar pattern in that the highest erosion rates occur downstream of the Highway # 103 bridge and above the Veteran's Memorial Bridge. Other areas along the main section of the waterfront show areas of less erosion and in some cases accretion. Much of the coastline along the waterfront is armored with large granite boulders to protect it from erosion. The analysis of the historic photos does reveal the low lying marsh land that was in filled in order to build the Bridgewater Mall. Based on the flood risk mapping that accounts for the combined effect of sea-level rise and storm surge through the use of adding a water level to normal high tide the mall is vulnerable to flooding along with some other sections of LaHave Street and Route 3 and the Shipyards Landing Park.

Due to the fact that the main developed waterfront of the town was most vulnerable to sea-level rise and storm surge, we executed our standard coastal GIS flood model approach based on still-water flooding. In this method, we assume the ocean water surface forms a horizontal plane that we raise to determine what areas are connected to the ocean and can be inundated. This technique has been used successfully and validated for many coastal areas that are adjacent to the ocean. We typically do not employ this method in a river domain where there is a distinct topographic gradient to the river, thus making the horizontal water level approach inappropriate. However, this GIS approach is much simpler and does not require the same degree of data requirements (e.g. bathymetry, and tidal and river boundary conditions). Thus as an experiment we generated flood layers from the still-water approach and compared them to the hydrodynamic approach for the maximum storm surge (3.5 m) simulations. A perspective view was generated to show the flood extent under normal high tide conditions, high tide plus a 2.2 m surge at the mouth of the LaHave, high tide plus a 3.5 m surge at the mouth of the LaHave,